Design Guidelines for Schematizing and Rendering Haptically Perceivable Graphical Elements on Touchscreen Devices

Hari P. Palani, Paul D. S. Fink & Nicholas A. Giudice

Taylor & Francis
Taylor & Francis Group

Check for updates

Design Guidelines for Schematizing and Rendering Haptically Perceivable Graphical Elements on Touchscreen Devices

Hari P. Palani ⬥, Paul D. S. Fink, and Nicholas A. Giudice

VEMI Lab & Spatial Informatics Program, School of Computing and Information Science, The University of Maine, Orono, Maine, USA

ABSTRACT
This paper explores the viability of new touchscreen-based haptic/vibrotactile interactions as a primary modality for perceiving visual graphical elements in eyes-free situations. For touchscreen-based haptic information extraction to be both accurate and meaningful, the onscreen graphical elements should be schematized and downsampled to: (1) maximize the perceptual specificity of touch-based sensing and (2) account for the technical characteristics of touchscreen interfaces. To this end, six human behavioral studies were conducted with 64 blind and 105 blindfolded-sighted participants. Experiments 1–3 evaluated three key rendering parameters that are necessary for supporting touchscreen-based vibro-tactile perception of graphical information, with results providing empirical guidance on both minimally detectable and functionally discriminable line widths, inter-line spacing, and angular separation that should be maintained. Experiments 4–6 evaluated perceptually-motivated design guidelines governing visual-to-vibrotactile schematization required for tasks involving information extraction, learning, and cognition of multi-line paths (e.g., transit-maps and corridor-intersections), with results providing clear guidance as to the stimulus parameters maximizing accuracy and temporal performance. The six empirically-validated guidelines presented here, based on results from 169 participants, provide designers and content providers with much-needed guidance on effectively incorporating perceptually-salient touchscreen-based haptic feedback as a primary interaction style for interfaces supporting nonvisual and eyes-free information access.

1. Introduction

The human sense of touch is one of our earliest senses to develop and works synchronously with other senses, such as vision and hearing (Maclean, 2008). Despite being an integral part of our perceptual experience in everyday life, the use of touch has traditionally been undervalued as a potential feed-back channel in computing devices as compared to visual or auditory information (Hayward et al., 2004). However, recent technological developments have spurred a significant increase in the use of haptic (active touch) feedback in human-computer interaction design. Advances in haptic tech-nology, both in hardware (touch input sensitivity) and soft-ware (gesture recognition) have been the primary drivers of the success of this important feedback mechanism and inter-action style (Bilton, 2013; Challis, 2013; Grussenmeyer & Folmer, 2017; Vatavu, 2017). Of note, the proliferation and growth of multi-touch touchscreen-based smart devices in the global market from 8.47 USD billion in 2018 to a predicted 22.33 USD billion by 2025 (representing a compound annual growth rate of 15.04%) has incentivized new ways to incorpo-rate touch in interaction design (Zion Market Research, 2019). Research efforts have demonstrated the advantages of utilizing touch as an interaction channel for both touchscreen-based input and output (I/O) operations. (Butler et al., 2016;

Mullenbach et al., 2014; Palani, Tennison, et al., 2018; Xu et al., 2011). Despite these efforts, almost all of the current interaction techniques and I/O operations on commercial touchscreen devices rely exclusively on visual feedback to guide movement and ensure accuracy. For instance, consider dialing a number or typing a text on a touchscreen interface. Although these interactions require touch-based inputs, the user interface (UI) elements are designed to require visual feedback to enable these interactions. The design and render-ing of such visual UI elements are governed by a set of human-interface guidelines and heuristics (such as optimal color for a button or optimal rendering size of an icon) that were established through empirical and usability studies, as well as by industry (Apple Human Interface Guidelines: Visual Design, 2019; Ng et al., 2011). Although an increasing interest in haptic capability has resulted in recent industry guidelines to ensure effective haptic operations ("Apple Human Interface Guideline: Haptics," 2020), these guidelines are intended for use in tandem with visual cues and are not designed to support nonvisual interactions that demand accu-rate tactual perception via haptic cues. As such, existing design logic, coupled with a lack of research emphasis and guidance on nonvisual interactions, has neglected a broad range of applications for this rapidly growing computing

CONTACT Hari P. Palani ✉ hariprasath.palani@maine.edu ⬥ VEMI Lab & Spatial Informatics Program, School of Computing and Information Science, The University of Maine, Orono, ME, USA

platform, especially in eyes-free use-case scenarios where visual feedback is either impractical or impossible.

One critical and well established application for eyes-free haptic interactions in computer interfaces is among people who are blind or have visual impairments (BVI) (Buzzi et al., 2013; Hayward et al., 2004; Sjostrom, 2001). Given the aging population in the United States, and that the prevalence of vision impairment increases with age, the benefits of nonvisual interactions can be conferred to older adults as well (Schieber, 2006). Visual impairments can also be situational, where a sighted person experiences temporary loss of vision that can include direct visual access to a touchscreen interface (e.g., due to glare or smoke or during operation of a vehicle). It is argued here that haptic feedback can serve as the primary interaction mode and that a better utilization of haptic interactions represent an excellent solution to these nonvisual use-cases. The goal of this paper is to establish the foundation for this hypothesis by aggregating and expanding critical design guidelines and specification parameters resulting from a rigorous series of empirical studies, pilot experiments, and conference papers by our research group. We aim for the outcomes of this research synthesis to provide guidance and specifications governing the adoption and implementation of haptic feedback and interactions that are foundational to nonvisual information access. By doing so, our guidelines will support the development of robust eyes-free information access techniques, increasing the accessibility and utility of these devices across diverse user groups and a broad range of touchscreen application scenarios. These application scenarios can be categorized into two major domains, namely: (1) applications involving situationally induced impairments and disabilities, and (2) applications involving multi-tasking.

1.1. Situationally-induced impairments and disabilities

Situationally-induced impairments and disabilities (SIID) are a prevalent (yet understudied) phenomenon in which users may experience situations that either temporarily obstruct visual cues to the user (e.g., glare and smoke) or limit the user from having direct visual access to the device's screen (e.g., use of a phone during a business meeting) (Barnard et al., 2007; Sears et al., 2003). Physical environmental factors such as lighting, rain, wind, and smoke are an important cause of situationally-induced visual impairment. Visual interaction on touchscreen-based displays depends on: (1) internal light from the device and (2) external light from the sun, lights, or the surrounding ambient environment. Users will find it difficult to perceive the on-screen content both when the internal light is too dim or when the external light is too bright, as this can cause reflection on the screen, a phenomenon commonly known as discomfort glare (Choe & Lee, 2015). Studies have demonstrated that glare caused by sunlight can affect user's cognitive performance, resulting in increased discomfort, especially for people already experiencing eye conditions such as photophobia (Rodriguez et al., 2016). On the other end of the luminance continuum, emergency management situations often require users to access maps and other important visually-oriented spatial information in situations dominated by unexpected loss of light from

power outages or for evacuation of a building due to fire or smoke (Monares et al., 2011). Similarly, owing to an explicit need for stealth in covert military operations, soldiers often must access information in a nonvisual mode, as using visual cues might reveal unwanted location information (Chiasson et al., 2003). Incorporating an eyes-free haptic-based mode of information access on the mobile device deployed in these situations could provide a simple and intuitive nonvisual solution for addressing these SIIDs. Similarly, social settings such as those dictating business etiquette, regulations governing behavior in polite society, cultural norms, use of discretion, and expectations from peers, all typically control when, where, and how mobile devices should be used (Abdolrahmani et al., 2016). Use of one's mobile phone while at a meeting is a common example of socially-induced SIID's. With purely haptic interactions however, which can be done nearly silently and without re-directing visual attention, a user could perform these tasks without disturbing others or being perceived as being rude, impolite, or distracted. Such haptic-based eyes-free interactions could also help the user to focus on social tasks by avoiding visual distraction.

1.2. Multi-tasking

One advantage of touchscreen-based computing is the ability for users to interact with highly adaptable and dynamic devices while simultaneously performing other operations. A typical example is manipulation of an in-vehicle infotainment display (e.g., interacting with control elements such as menus, buttons, and scroll bars) while also operating a vehicle. Although manipulation of in-vehicle entertainment systems can be effectively achieved by mechanical and manual controls, these physical solutions are quickly being replaced by touchscreen-based interfaces in order to leverage increased adaptability and flexibility. Indeed, simultaneously interacting with these interfaces while driving can be dangerous and even life threatening, as the driver's visual attention can shift from the primary task of seeing the road to accessing control elements on an interface (Swette et al., 2013). According to the AAA Foundation for Traffic Safety, up to 60 percent of teen car crashes are caused by driver distraction, with many of these drivers' distractions resulting from looking at/operating/manipulating infotainments systems, dashboards, and climate controls (Carney et al., 2016). Similarly, a study published by ABI Research suggests that automotive infotainment systems cause a significant cognitive overload for users while driving (Vatavu, 2017). It is argued here that eyes-free interactions based on haptic and multimodal touchscreen interfaces, as we are studying, could provide a viable solution by acting as the primary feedback channel for interaction with such infotainment systems, thereby leaving the driver's visual attention focused on the primary task of safely operating the vehicle. Imagine the same situation where the driver could manipulate the controls solely by using haptic (or combined haptic and audio) feedback without having to divide/distract their visual attention from the road. Research on multi-tasking while driving has suggested that safety and driving performance increases in the presence of multimodal feedback (Pitts et al., 2012; Shakeri et al., 2016; Swette et al., 2013; Wickens

& Seppelt, 2002). This advantage conferred by the presence of haptic feedback is not only true for driving scenarios, but also holds for several other multi-tasking situations, such as walking or jogging while operating music controls on a smartphone (Challis, 2013; Leung et al., 2007). We argue that off-loading the visual information being displayed on the touchscreen to a touch-based sensory channel will increase cognitive and attentional resources, thereby reducing the risk of accidents by allowing users' visual attention to remain on the critical task (i.e., watching their walking or running path).

2. Challenges in incorporating haptic feedback for nonvisual information access on touchscreen devices

For any nonvisual graphics access solution to succeed, it is of the utmost importance that the original visual graphical material is schematized and rendered based on parameters that support the sensory, perceptual, and spatio-cognitive characteristics of the sensory channel to which it is being delivered. As such, our focus in this work is geared toward the state space of different eyes-free situations experienced by multiple populations, i.e., situational impairments faced by sighted users and health/sensory induced impairments faced by BVI users. To this end, this paper investigates the key perceptual and cognitive characteristics underlying haptic interactions that are pertinent to touchscreen-based haptic (vibrotactile) feedback.

Whether the need for nonvisual touchscreen use is due to multitasking, situationally induced impairments and disabilities, or visual impairment more generally, simply substituting haptic cues for visual or audio cues to perform I/O operations will not be meaningful to users unless the information being rendered and presented is optimized to support the specificity of tactual information processing. For instance, an exact haptic analog of a visually-rendered graphical element will not be meaningful in the vast majority of cases, as vision is estimated to have 500 times greater sensory bandwidth than touch (Loomis et al., 2013). Despite any inherent differences in sensory bandwidth, substituting touch cues for visual cues will be most meaningful to users when the presented information is first optimized to support the perceptual and cognitive characteristics of tactual sensing and haptic information extraction. Indeed, if this sensory-specific optimization is considered as part of the design process, nonvisual modalities can be used as effectively as visually-mediated interactions. In support, spatial updating performance after touch-based learning of various stimuli, such as tactile maps or object arrays, yielded functionally equivalent performance on learning and updating tasks as was observed on the same tasks after visual learning of identical stimuli (Giudice et al., 2011; 2009). Functional equivalence of multisensory information processing/representation in the brain provides a theoretical underpinning for why haptic interactions can substitute for visual interaction design and use of interactive interfaces, as we are advancing here. Further evidence supporting this theory and the importance of multimodal human information processing comes from educational contexts. Several researchers have established the importance of incorporating multimodal cuing in educational settings and have demonstrated improved learning efficacy, including that of microspatial properties like patterns and compliance, using haptics (Barfield, 2009; Grow et al., 2007; Sathian, 1998). Unlike the aforementioned efforts, the challenge in presenting tactile information on touchscreen interfaces is aggravated, as touchscreens do not provide any explicit cutaneous cues on the finger(s) except for the perception of a flat, featureless glass surface. The tactual component of touchscreen-interfaces is almost exclusively limited to input, with very little traditional cutaneous feedback, e.g., as one would obtain from the fingertip when feeling most other types of textured, ridged, or otherwise haptically salient surfaces. To overcome this absence of intrinsic cutaneous cues, and to facilitate access to on-screen control elements, touchscreen-based haptic interactions must rely on extrinsic haptic feedback (e.g., vibration, friction, or electrostatic cues) and kinesthetic hand movement during screen exploration. This means that perceiving digital information on a touchscreen display with extrinsic feedback such as vibration or friction is very different from perceiving information with vision or perceiving traditional tangible media (O'Modhrain et al., 2015; Tennison & Gorlewicz, 2016). For accurate perceptual interpretation of the graphical elements using touchscreen-based haptic/vibrotactile feedback, users must follow a three-step process: (1) employ proprioception (i.e., force, position, and motion sensing) to keep track of their finger position within some frame of reference, defined by the body or an external reference such as the display frame, (2) extract the spatial information by synchronously interpreting the vibrotactile cues, and (3) interpret the on-screen element by associating the perceived sensory information with the on-screen interface element (Klatzky et al., 2014; Palani & Giudice, 2017). For haptic information extraction to be most accurate and meaningful, the onscreen graphical elements should be schematized based on: (1) the perceptual specificity of touchscreen-based haptic feedback, and (2) the technical limitations of the interface that demands users to actively perform this three-step process.

Vibrotactile/haptic interaction, as is required on touchscreen devices, is an effective approach for replacing traditional embossed/raised tangible media designed to support blind and visually-impaired (BVI) users (Giudice et al., 2012). To govern and guide such applications, several standards and guidelines have been established for producing tangible graphics using hardcopy output produced by tactile embossers, microcapsule swell paper, and even for custom handmade graphics (Braille Authority of North America, 2010; Rowell & Ungar, 2003). Although these guidelines support the design of perceptually salient tangible graphics, they do not translate well to rendering digital graphical elements. This is because the perception of raised tangible media involves different stimuli and physical processes than are required for haptic touchscreen-based interactions enabled by vibrotactile sensation. While tactual perception of both types of stimuli inevitably involves multiple classes of mechanoreceptors and overlap of the neural channels mediating this information, based on what combinations of spatial, temporal, and thermal properties are present (Bolanowski et al., 1988), traditional embossed/raised tactile stimuli and

the vibrotactile stimuli we studied here most likely utilize different fundamental receptor types. For instance, cutaneous stimulation from pressure-based *mechanoreceptors* on the fingertip from deformation caused by contact with vibrating stimuli on a flat touchscreen will be much less than would be elicited from activation of these receptors by skin displacements from finger movement over traditional embossed stimuli (Klatzky et al., 2014). By contrast, the touchscreen-based vibrotactile stimuli used here were likely prioritizing activation of Pacinian corpuscles in addition to pressure-based *mechanoreceptors* as the Pacinians are most associated with vibration and vibrotactile stimulation, with their peak sensitivity between 200 and 300 Hz (Loomis & Lederman, 1986). As the majority of vibration motors and actuators used in commercial smart devices operate around 250 Hz (Choi & Kuchenbecker, 2013), it is likely that the touchscreen-based haptic information extraction that occurred in these studies via the above-mentioned three-step process was primarily activated by these receptors. Therefore, the existing guidelines established to ensure perceptibility and salience based on the traditional pressure-based deformations and skin displacements required to perceive embossed stimuli and tangible graphics are not necessarily transferable to vibrotactile rendering of digital graphical elements, where perception occurs via a featureless flat screen and significant Pacinian innervation. While there is an active research area investigating parameters and guidelines for authoring graphical elements to support touch interactions in conjunction with visual access, no work to our knowledge has systematically investigated or rigorously identified the perceptual parameters for governing and supporting eyes-free touch (haptic) interactions.

The studies that have evaluated the usability of touchscreen-based interfaces as a nonvisual graphical access solution have all utilized different parameters for their evaluations. For instance, a target size of ~0.17inch was used in the *Timbremap* project for map exploration using an iPhone (Su et al., 2010). A rendering width of ~0.35inch (which is 8 times the size of traditional embossed graphics) was utilized as the optimal line width for rendering and accessing shapes, graphs and maps using a Vibro-Audio Interface (VAI), similar to the system studied here, on a 7.0inch android galaxy tablet (Giudice et al., 2012; Palani, 2013; Raja, 2011). A rendering width of ~0.20 inch was used for shape identification in the GraVVITAS project, which used a Dell Latitude XT Tablet as the rendering platform (Goncu & Marriott, 2011). Similarly, Tennison et al., compared a width of ~0.15inch to ~0.31inch in a shape identification task and found that users were able to identify smaller shapes with a thin border (0.15inch) at rates comparable to those with 0.31inch borders, after first being exposed to the larger shapes (Tennison & Gorlewicz, 2016). Such unguided use of random parameters has limited the scope and usability of these promising approaches. Without guidelines and empirical investigation of optimal rendering sizes and information density on touchscreens, designers run the risk of depreciating user experience, and consuming unnecessary screen space, which could lead to increased effort in information extraction. Furthermore, rendering content at too small of a size, potentially sub-threshold, may not support users with accurate perception of on-screen information, leading to the failure of the approach being advanced.

2.1. Current research

If research in touchscreen-based tactual information processing is to succeed, a principled research approach that streamlines and codifies foundational features of the underlying graphical information is necessary. As such, the intent of this work is not to cover all aspects of this new research area, or to address all features of graphical information access. Rather, the investigation presented here was streamlined to focus primarily on the rectilinear line (and polyline) features of graphical materials (e.g., bar graphs, line graphs, subway/metro maps, electrical circuits, etc.). It is argued here that these features are an appropriate starting point for this foundational research, as lines are a crucial spatial construct for rendering the majority of graphical content, such as graphs and maps. The rationale for this specification and research focus is not only to reduce the state space of the underlying graphical elements evaluated in this work, but also to illuminate characteristics of a core graphical component that can serve as a building block for extending the investigation to other components such as regions (e.g., states or provinces in a map where the boundary is indicated as a line). With this guiding focus, three initial experiments were conducted to investigate and identify the minimum line width for detecting on-screen vibrotactile lines (Exp-1), the minimum interline gap width for discriminating vibrotactile lines rendered parallel to each other (Exp-2) and the minimum interline gap width for discriminating oriented vibrotactile lines (Exp-3). The sample size for each experiment was determined using the G*Power calculator via a priori power analysis (based on an alpha of 0.05, an expected power of 0.95, and an effect size of 0.25 as suggested by (Cohen, 1988; Faul et al., 2007). All three experiments were approved by the Institutional Review Board (IRB) of the University of Maine and written informed consent was obtained from all participants.

3. Experiment 1: Vibrotactile line detection

The ability to detect graphical lines (e.g., each path on the transit map in Figure 1) using vibrotactile feedback represents a critical first step toward apprehension of global graphical content via nonvisual access on touchscreen-based interfaces. For instance, imagine accessing the transit map in an eyes-free setting using only touchscreen-based vibrotactile feedback. Detecting individual subway paths (i.e., lines) represents the first step toward accessing and understanding global information about the subway map. To support comprehension of graphical information, each vibrotactile line must be rendered at a minimum width that not only supports its detection but should also preserve the spatial structure and topology of the original visual graphical rendering. To this end, Experiment 1 was designed to identify the minimum line width that should be used for rendering haptically perceivable graphical lines.
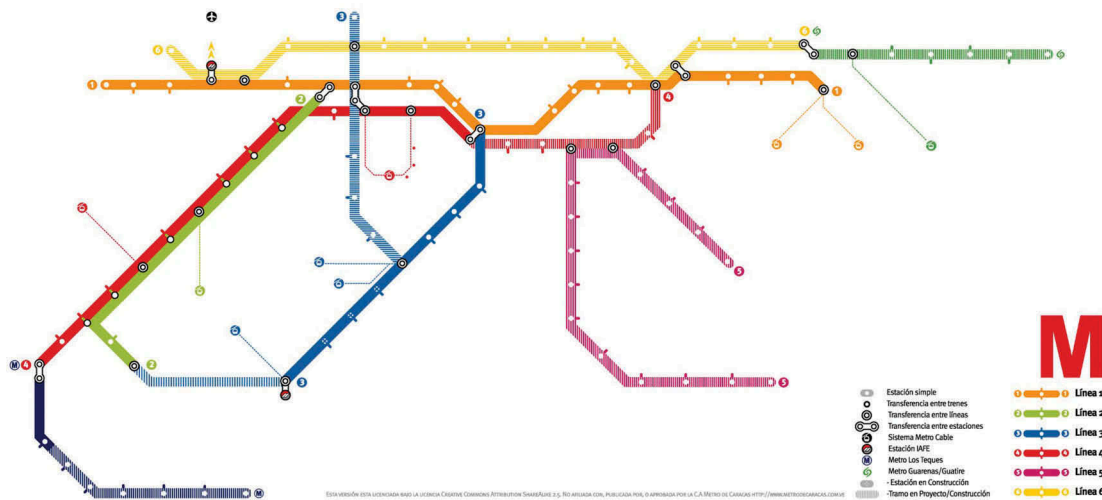
Figure 1. An exemplary transit map.

3.1. Method

Fifteen blindfolded-sighted participants (7 females and 8 males, ages 19–32) and twenty blind and visually-impaired (BVI) participants (9 males and 11 females, ages 21–74, BVI demographic details are presented in Appendix A) were recruited for this experiment. The stimulus set consisted of seven different line widths (0.125, 0.25, 0.5, 1, 2, 4, and 8 mm). These line widths were chosen because the smallest width of 0.125 mm was approximately equivalent to the size of a single pixel on most current touchscreen displays. From this base, the stimuli was increased linearly by a factor of 2 up to 8 mm, which is known from previous studies to be equivalent to the size of the contact patch of the index finger, the most commonly used finger for touchscreen-based interactions (Giudice et al., 2012; Palani & Giudice, 2014, 2017). The stimuli were presented using the prototype vibro-audio interface (VAI) implemented on a 5.6inch Galaxy Note4 Edge Android phablet (Palani, 2013). Whenever an onscreen rendered graphical line was touched by the user, the device's vibration motor was triggered to provide a constant vibration (based on Immersion Corp's UHL effect "Engine1_100" – an infinite repeating loop at 250 Hz with 100 percent power), creating the perception of focal vibrotactile stimulation on the user's finger (Immersion Corp, 2019). The device comes with two feather touch buttons that do not provide any tactile feedback. To avoid potential errors or interruption during experimental trials, these buttons were covered with Velcro straps (see Figure 2). In addition, the device comes with an edge screen that acts as a standalone secondary touchscreen. This side screen was used by the experimenter as the controlling area for quickly manipulating experimental trials without distracting the participant from his/her experimental tasks.

3.2. Procedure

The study followed a within-subject design with each participant performing 84 line counting trials (resulting in 360 observations for each tested line width). A trial rendered 1, 2, or 3 lines on the screen, with all lines being of the same
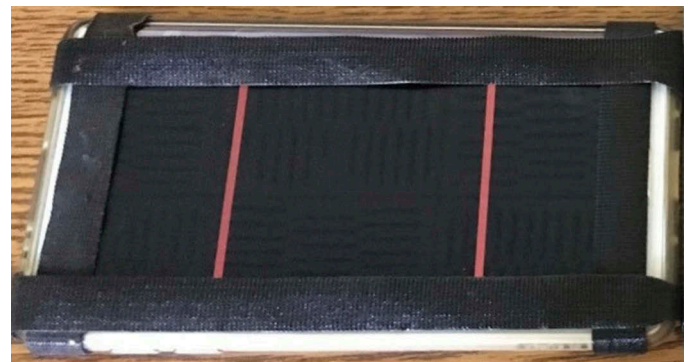

Figure 2. Randomly generated lines rendered on the galaxy note4 edge phablet for Experiment 1.

width per trial. The lines were randomly generated and were evenly spaced for the two-line (~850 pixels/1.6 inches apart) and three-line (~640 pixels/1.2 Inches apart) trials. The detectable line width of vibrotactile line was evaluated using a move/scan gesture as opposed to static finger/device position. The rationale for evaluating the vibrotactile line width using a move/scan gesture is motivated by nonvisual user interaction techniques (i.e., exploratory procedures) followed by visually-impaired users. These techniques include employing a zig-zag motion when line following/tracing, circling around an intersection, contour following using the device edge as a reference, and four-directional scanning around an intersection (Palani, 2013, 2018; Raja, 2011). A constant motion was used in each trial to identify a conservative value of the width needed for accurate detection of vibrotactile lines across different exploratory procedures. We postulate that if a line can be detected using this conservative, consistent (fixed-speed) scan, it will be detectable when using the nonvisual user interaction techniques (i.e., exploratory procedures) often employed by BVI individuals, including zig-zag motions, circling, contour following using the device edge as a reference, and four-directional scans (Raja, 2011). Accordingly, in each trial, participants were asked to swipe their finger across the screen from left to right at a constant

speed and to verbally indicate the number of vibrotactile lines perceived during this scan upon its completion. Once participants indicated the number of lines, the experimenter quickly changed the stimuli using the side screen and the change was indicated to the participant via speech message stating "Next". The participant then brought their finger back to the left side of the screen and began the next trial following the same procedure. Participants were provided with practice trials to get acquainted with the experimental device and practice scanning in a consistent manner. The experimenter ensured that they maintained the scan speed during both the practice and test trials. Participants took between 15 and 30 minutes to complete the entire experiment with per trial scan time ranging between ~1.4 and ~3.5 seconds. Based on this design, line detection accuracy was compared within subjects across the seven line widths and between subjects for the 2 participant groups (sighted vs. BVI).

3.3. Results and discussion

The accuracy in line detection was compared using a (7x2) mixed model ANOVA, with the seven line widths as within-subjects factors and the two participant groups (sighted versus BVI) as independent factors. Results revealed a significant difference in line detection across the seven line widths ($F(6, 198) = 280.776$, $p < .001$), but no reliable differences were observed between the two participant groups ($F(1, 198) = 1.609$, $p > .05$) or the interaction between the line widths and the participant groups ($F(1, 33) = 1.612$, $p > .05$).

Post-hoc paired sample t-tests, using Bonferroni correction, indicated that the detection accuracy with line widths 0.125, 0.25 and 0.5 mm were significantly different from each other and exhibited significantly lower detection accuracy than the remaining four line widths (see Table 1 for means and SDs and Table 2 for p values). However, there were no statistically significant differences observed between detection of line widths 1, 2, 4, and 8 mm (see Table 2 for p values). These results indicate that rendering graphical lines at a width of 1 mm is sufficient for tasks requiring simple line detection via vibrotactile cuing. While designers tend to adhere to the motto "bigger is better", results here demonstrate otherwise. While rendering lines at widths 0.5 mm can maximize screen space and provide ~75% accuracy, this comes at the cost of reduced detection accuracy, which is neither a wise design decision nor acceptable for use in real-world applications. The rationale for adopting such a psychophysically-motivated usability evaluation paradigm is to not only achieve perceptual saliency, as would be identified via traditional psychophysical procedures (i.e., at least ~75% accuracy), but is also to identify a parameter that is functional for usage in practical scenarios. That is, when implemented, line width should enhance the overall usability and utility of the interface. Based on this logic, a 1 mm line width (which led to a 97% detection accuracy) is suggested here as the minimum line width that best supports reliable detection of vibrotactile lines. While adopting a line width wider than 1 mm may improve saliency and ensure 100% accurate detection, doing so will consume more screen space than necessary. Designers should carefully consider the tradeoff between employing the 1 mm

guideline, as empirically determined here. Depending on the criticality of the task that could demand 100% detection accuracy, the line width can be increased to higher values (i.e., 2 mm or more) at the cost of losing screen space. It should be noted that the suggested guideline of using a 1 mm line width pertains only to detection of graphical lines using vibratory cues and not to more complex perceptual tasks, such as line tracing and contour following, which are evaluated in experiments 4–6.

4. Experiment 2: Vibrotactile gap detection

Almost all visual interface elements are composed of multiple lines rendered in close proximity to each other. As shown in Figure 1, to be recognized as a distinct transit line, each of the individual lines must be separated from its neighboring adjacent line by an interline gap wider than the minimum perceivable gap width. Given the sparse spatial resolution of touch, if the transit lines in this example were to be rendered in their original form for nonvisual access on touchscreen displays, users would be unable to discriminate them via haptic cues. On the other hand, rendering the lines using too large of an inter-line gap is also a poor design decision, as it will needlessly consume valuable display space. In addition to the actual interline-gap, the width of the bounding vibrotactile lines can also influence the perception of the gap between them. This is because of the lag in generation and perception of vibrotactile feedback on touchscreen devices. This lag was attributed by two factors: (1) lag from vibratory motors and (2) the device's computational capacity. Vibratory motors on even the most modern commercial touchscreen-based devices utilizing linear resonant actuators (LRAs) as was the case on our test devices, suffer from slight computational and start/stop lag between triggering and stopping the actuators. This "rise time" or "start-up time" as it is often referred, can vary between devices, such as Precision Microdrives' 12 mm LRA at ~18 ms rise time (Precision Microdrives, 2016) and Texas

Table 1. Mean line detection accuracy across tested line widths and participant groups.

Line Width (in mm)	Sighted		Blind	
	Mean (%)	SD	Mean (%)	SD
0.125	21	40.9	26	44.2
0.25	35	47.8	47	50
0.5	75	43.4	76	42.9
1	97	18	98	15
2	100	0	100	0
4	100	0	100	0
8	100	0	100	0

Table 2. P-values for paired sample t-tests comparing the seven line-widths.

Line Width (mm) (in mm)	0.125	0.25	0.5	1	2	4	8
0.125	NA	0.00	0.00	0.00	0.00	0.00	0.00
0.25	0.00	NA	0.00	0.00	0.00	0.00	0.00
0.5	0.00	0.00	NA	0.00	0.00	0.00	0.00
1	0.00	0.00	0.00	NA	1.00	1.00	1.00
2	0.00	0.00	0.00	1.00	NA	1.00	1.00
4	0.00	0.00	0.00	1.00	1.00	NA	1.00
8	0.00	0.00	0.00	1.00	1.00	1.00	NA

Instruments' estimate of 40–60 ms LRA start-up time (Rao, 2012). Furthermore, the device's computation time for calculating the centroid pixel from users touch and simultaneously triggering the actuators is ~10 ms (as estimated from device's event log during our pilot testing). Although minimal, this computation lag (~10 ms) in conjunction with the mechanical lag from the motor (~10 ms) becomes a perceivable lag for users, given that the mean scan time per trial in experiment 1 was estimated to be ~2 seconds. This lag causes a spurious perception of a line being wider than its actual size, masking the gap and resulting in two lines being incorrectly perceived as one. For accurate vibrotactile discrimination of graphical lines, the inter-line gap must be greater than the minimum perceptible width to avoid such spurious haptic perceptions. Accordingly, Experiment 2 was designed to identify the minimum interline-gap width that supports discrimination of two or more vibrotactile lines (rendered parallel to each other) while also evaluating whether the bounding line width may cause erroneous haptic perception due to the lag in vibrotactile feedback imposed by the device.

4.1. Method

Eighteen blindfolded-sighted participants (9 females and 9 males, ages 19–33) and eighteen blind and visually-impaired (BVI) participants (7 males and 11 females, ages 20–74, BVI demographic details are presented in Appendix A) were recruited for this experiment. The stimulus set consisted of five gap widths (i.e., 0.25, 0.5, 1, 2, and 4 mm). The gap widths were chosen such that 1 mm (as was found in Experiment 1) was kept as the median value and increased (or decreased) by a factor of two. The apparatus, implementation, and procedure were similar to that of Experiment 1 (Figure 3). To assess the possible effect of spurious haptic perception and to better characterize and understand the relation of line width on gap detection accuracy, the five gap separations were tested across three different line widths (i.e., 1, 2, and 4 mm).

4.2. Procedure

The study followed a within subject design, with each participant performing 54 line counting trials (resulting in 162 observations for each tested gap width for each participant

Figure 3. Randomly generated lines rendered on the galaxy note4 edge phablet for Experiment 2.

group). A gap trial rendered 1, 2, or 3 pairs of lines with each pair separated by a set gap width. The line widths and gap widths were held constant within each trial. In each trial, participants were asked to move their finger across the screen from left to right at a constant speed, to count the vibrotactile lines perceived during the scan, and to verbally indicate this number to the experimenter upon completing the trial. To confirm that participant responses were based on gap detection (and not guesses), 9 dummy trials (i.e., trials where the rendered stimuli did not have interline gaps) were added to the 45 gap detection trials, resulting in 54 line counting trials. Each participant took between 20 and 30 minutes to perform the 54 trials. Based on this design, the accuracy in gap detection was compared for both blindfolded-sighted and BVI participant groups as a function of: (1) five gap widths (i.e., space between a pair of lines), and (2) three line widths.

4.3. Results and discussion

The accuracy in gap detection was compared using a (5x2) mixed model ANOVA across the five tested gap widths as the within-subjects factor and the two participant groups (sighted versus BVI) as independent factors. Results revealed that there was a significant difference in detection across the five gap widths ($F(4, 136) = 73.032$, $p < .001$), but no reliable differences were observed between participant groups ($F(1, 34) = 0.397$, $p > .05$) or the interaction between the gap widths and the participant groups ($F(4, 136) = 0.790$, $p > .05$). Subsequent post-hoc paired sample t-tests, using Bonferroni correction, indicated that the gap widths 0.25 and 0.5 mm were significantly different in detection accuracy from each other and exhibited significantly lower detection accuracy than the remaining three gap widths (see Table 3). Similarly, the accuracy in gap detection was compared using a mixed model (3x2) ANOVA across the three tested line widths as a within-subjects factor and the two participant groups (sighted versus BVI) as independent factors. Results revealed a main effect of line width ($F(2, 68) = 60.417$, $p < .001$), but no reliable differences between the participant groups or the interaction between the line widths and the participant groups (see Tables 4 and 5) (all $ps > 0.05$).

Table 3. Mean gap detection accuracy for the two participant groups as a function of gap width.

	Blindfolded		Blind	
Gap Width (in mm)	Mean (%)	SD	Mean (%)	SD
0.25	37	48.4	43	49.7
0.5	55	49.9	63	48.4
1	68	46.8	73	44.6
2	78	41.7	79	40.8
4	91	28.2	91	30.7

Table 4. P-values for paired sample t-tests comparing the five gap-widths.

Gap Width (in mm) (in mm)	0.25	0.5	1	2	4
0.25	NA	0.000	0.000	0.000	0.000
0.5	0.00	NA	0.009	0.000	0.000
1	0.000	0.000	NA	0.192	0.000
2	0.000	0.000	0.192	NA	0.005
4	0.000	0.000	1.000	0.005	NA

Table 5. Mean gap detection accuracy for the two participant groups as a function of tested line widths.

	Sighted		Blind	
Line Width (in mm)	Mean (%)	SD	Mean (%)	SD
1	49	50.1	53	50
2	65	47.8	69	46.4
4	84	37	87	34.1

Subsequent post-hoc paired sample t-tests with Bonferroni correction indicated that accuracy with the three line widths increased linearly with a corresponding increase in line width and were all significantly different from each other (Table 4). Of the tested gap widths, only the 2 mm and 4 mm gaps exhibited an overall detection accuracy greater than is required by traditional psychophysical procedures (i.e., 75% detection accuracy). However, further analysis including the line widths revealed that the two gap widths (i.e., 2 mm and 4 mm) exhibited greater than 90% detection accuracy when coupled with a 4 mm line width, as opposed to 87% with 2 mm bounding lines and 74% with 1 mm bounding lines. These findings suggest that the ability to accurately discriminate parallel vibrotactile lines is not only dependent on the width of the interline gap but also on the width of the bounding vibrotactile lines. Given that the perception of narrower line widths and gaps can be impacted by the lag (~20 ms in this case) created by the device's computation for calculating the centroid point of the touch location, triggering the actuator, and the start/stop time of the actuator itself, line and gap width parameters should not be treated separately when creating/authoring vibrotactile graphical information. We recommend that the width of bounding lines should be increased depending on the width of the interline gap. Although the overall (end-to-end) lag time varies from device to device, dependent on its computational capabilities and type of vibration motor used, this recommendation holds true for most of the advanced touchscreen-based devices, as even minimal lag can significantly impact users who employ a faster scanning strategy. Thus, designers should carefully choose a line/gap width combination that provides the best trade-off between accuracy and screen space.

As stated earlier, the aim for these studies is to achieve as close to 100% detection accuracy such that it supports practical usage in common scenarios. Based on this intent, a 4 mm interline gap width bounded by vibrotactile lines of width 4 mm (which led to ~96% detection accuracy) is suggested here as the minimum line width and gap width that best supports detection and discrimination of parallel vibrotactile lines. As stated in Experiment 1, designers must decide the rendering parameters based on the task at hand. If the task demands accurate gap detection at a lower line width, then the gap width can be increased to values greater than 4 mm, at the cost of losing screen space. It should be noted that this suggested guideline pertains only to detection and discrimination of parallel vibrotactile graphical lines and not for lines oriented at angles, as are evaluated in the following experiment.

5. Experiment 3: Discriminating oriented vibrotactile lines

As discussed earlier, with the extrinsic cuing mechanism employed on touchscreen devices, users can only detect whether the touched location is on or off (i.e. feel if it is vibrating) but they cannot directly perceive any other meaningful stimulus information, such as its width/length/angle without active finger movements. To extract meaningful information using such an extrinsic feedback mechanism, as is required for use on touchscreen devices, users must perform exploratory procedures (EPs), which are a stereotyped pattern of manual exploration observed when people are asked to learn about a particular object property during voluntary manual exploration without vision (Lederman & Klatzky, 1987; Loomis & Lederman, 1986). While Experiments 1 and 2 established the minimum line and gap widths for detection and discrimination of parallel vibrotactile lines, it is not clear whether these parameters are generalizable to oriented vibrotactile lines and angular graphical elements (for example, see the red and blue transit lines in Figure 1). For identifying such oriented lines and judging the angle subtended between them, BVI users will typically employ a "circling" strategy (see Figure 4 left), where they move their finger in a circular pattern around the intersection as their exploratory procedure (Palani et al., 2016; Palani, 2013; Palani & Giudice, 2017; Raja, 2011). Based on this exploration strategy, the arc of the circle (see Figure 4 left) formed during the act of executing the circling EP represents the interline gap for oriented vibrotactile lines. From a geometric standpoint, the straight-line distance (see Figure 4 right) between two oriented lines is the cord length (cord length = $2\,r\,\sin(\theta/2)$). It is postulated here that this cord length (and by extension the angular separation, i.e., the arc length) should be wider than the minimum perceivable gap width for supporting accurate discrimination of adjacent oriented vibrotactile lines emanating from an intersection/vertex.

The cord length is a variable that depends on: (1) θ – angle subtended between the lines, (2) r – the radius of the traced circle, or (3) both 1 and 2. In theory, the 4 mm gap width identified in Exp-2 should be translated into a 4 mm cord length for accurate detection of distinct oriented lines.
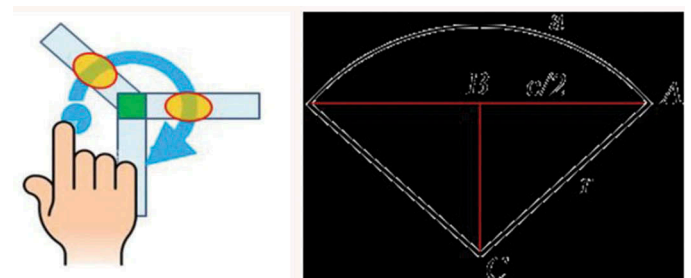

Figure 4. (left) Intersection circling strategy: Adapted from (Raja, 2011), (right) Geometric representation of cord length "c" and radius "r".

However, the cord length cannot be fixed at a constant value as it varies depending on the angle (θ) subtended between oriented vibrotactile lines and the radius (r) of the circle formed by the user while performing the "circling" exploratory procedure. For instance, at a circle radius of 1-inch and a 4 mm cord length, the user can (in theory) discriminate oriented lines separated by an angular magnitude of 5°, but by increasing their radius to 2-inches, they should be able to discriminate oriented lines separated by an angular magnitude as low as 2°. Acknowledging the dependency between these three variables, Experiment 3 was designed to identify the minimum cord length that supports detection and discrimination of oriented vibrotactile lines.

5.1. Method

Eighteen blindfolded-sighted participants (9 females and 9 males, ages 19–34) and eight BVI participants (3 males and 5 females, ages 25–74, BVI demographic details are presented in Appendix A) were recruited for this experiment. The stimulus set was designed as a simple line layout where multiple lines were converging to/diverging from an intersection point at the center of the screen (Figure 4). The number of lines in each stimulus set ranged from 5 to 9 based on Miller's "The Magical Number Seven, Plus or Minus Two" (Miller, 1956). To evaluate the influence of radius in supporting discrimination of oriented lines, two conditions were designed and evaluated. The radius was set as a constant value of 1-inch and 2-inch for conditions 1 and 2 respectively. At a radius of 1-inch from the vertex/intersection, the minimum gap width of 4 mm (i.e., cord length in this context) was translated to an angular magnitude of ~9°. Similarly, at a 2-inch radius, the gap width of 4 mm was translated to a ~ 5° angular magnitude. To evaluate the influence of cord length (i.e., actual gap) on the discrimination of oriented lines, two additional angles (2° and 22°) were also added to the stimulus set that approximately translated to the 4 mm gap width at a radius of 0.5-inch and 4-inch (meaning the radius of the two primary conditions increased and decreased by a factor of 2). Similar to previous experiments, the stimuli were presented using our prototype VAI (Palani, 2013) implemented on a touchscreen equipped tablet computer – 10.1 inch Galaxy Table 3. For controlling the circle radius in each condition and for assisting users with the circling strategy, two circular paper stickers of 4 mm width (one at 1-inch from the center and the other at 2-inches from the center) were affixed on the screen (see Figure 5). In addition, the intersection point (center of the screen) was also demarcated with a paper sticker of 10 mm radius. To assist participants with orienting themselves on the screen, each circle had a start point (indicated by a tactile marker at the 5 o'clock position).

5.2. Procedure

The study followed a within-subjects design, with each participant performing 28 line counting trials in each circling condition (resulting in 180 observations for each tested angular magnitude). A trial rendered 5, 6, 7, 8, or 9 lines on the screen each of width 4 mm (for example, see Figure 5). The
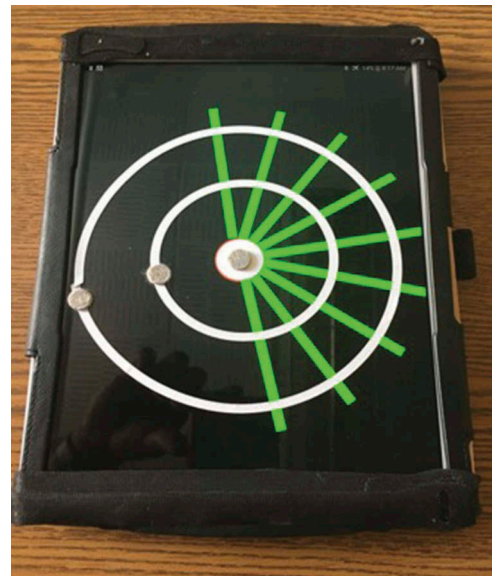

Figure 5. Experimental device with circular stickers for two radii and tactile markers denoting the start points.

lines were indicated via a constant vibration based on Immersion Corp's UHL effect "Engine1_100" – an infinite repeating loop at 250 Hz with 100 percent power (Immersion Corp, 2019). In each trial, the angular magnitude between adjacent lines was kept constant irrespective of line number. The order of the conditions (1-inch versus 2-inch radius) was balanced across the participants and the order of stimuli presentation in each condition was randomized within the script. In each trial, participants were asked to start at the reference start point (indicated by a tactile marker) and to count the number of lines perceived in a full 360°circuit by tracing along the circular path (either at a 1-inch or 2-inch radius depending on the condition). Upon returning to the start point, they lifted their finger from the display and verbally indicated the number of lines perceived during the 360° scan. Each participant took between 20 and 40 minutes to complete the entire experiment.

5.3. Results and discussion

Accuracy in oriented line detection was compared using a (4x2) mixed model ANOVA across the four tested cord lengths as a within-subjects factor and the two participant groups (sighted versus BVI) as independent factors. Results revealed a main effect of cord length both, for inner circle: (F (3, 72) = 10.85, p < .001), and for outer circle: (F(3, 72) = 12.345, p < .001). But no reliable differences were observed between the participant groups or the interaction between the cord lengths and the participant groups (all ps > 0.05).

Subsequent post-hoc paired sample t-tests based on Bonferroni correction indicated that for both circling conditions accuracy in line detection for trials with cord lengths 4 mm and below were significantly lower when compared with cord lengths greater than 4 mm (see Table 6). But there were no significant differences in line detection accuracy for
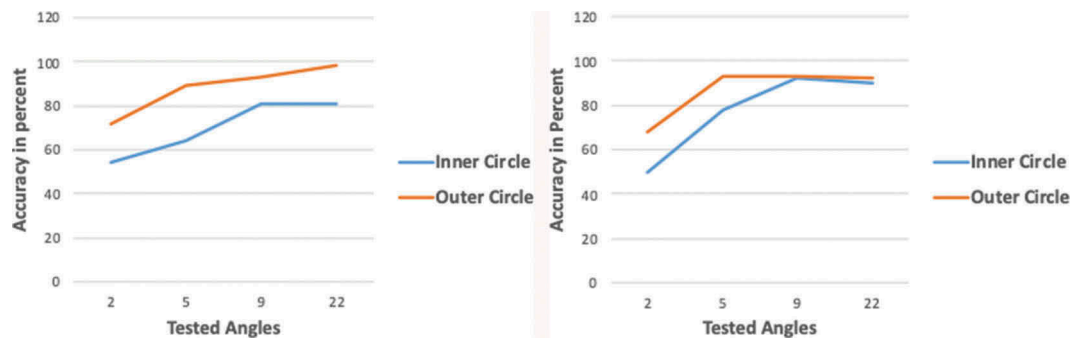
Figure 6. Oriented line detection accuracy as a function of four tested angles and two circling conditions for the sighted group (left) and the BVI group (right).

Table 6. P-values for paired sample t-tests comparing the four tested angles and two circling conditions.

Angles (in degrees)	1-inch circling condition				2-inch circling condition			
	2	5	9	22	2	5	9	22
2	NA	0.005	0.000	0.000	NA	0.000	0.000	0.000
5	0.005	NA	0.011	0.000	0.000	NA	0.667	1.000
9	0.000	0.011	NA	0.956	0.000	0.667	NA	1.000
22	0.000	0.000	0.956	NA	0.000	1.000	1.000	NA

the trials with cord lengths greater than 4 mm (i.e., 9°, and 22° for 1-inch and 5°, 9°, and 22° for 2-inch). This finding indicates that a 4 mm cord length is sufficient to accurately detect and discriminate oriented vibrotactile lines when using a "circling" strategy. This parameter is in line with the results found in Exp-2, which established a 4 mm gap width for accurate detection of parallel vibrotactile lines. It should be noted that these findings are pertinent only to the current context of using a "circling" strategy for identifying oriented lines emanating from an intersection. While it is argued here that this is the best strategy to use, the results are not necessarily generalizable to other/all tactual learning/tracing strategies.

6. Building mental representations of graphical information via haptic perception

For comprehending the global spatial information of graphical materials such as the transit map shown in Figure 1, users must use "line tracing" behavior in addition to detection and discrimination of individual line segments. The term "line tracing" is commonly referred to in the literature as "contour following", which is a type of exploratory procedure utilized for identifying object properties during haptic exploration

(Klatzky et al., 2014; Lederman & Klatzky, 2009). For traditional tangible graphics, *contour following* means tracing an edge *(i.e., line)* on a raised-line drawing or tactile map using cutaneous perception on the finger digit. However, such cutaneous perception is not applicable for touchscreen-based haptic interactions. Thus, in the context of the current evaluations, the term "line tracing" is defined as the exploratory procedure that is used for following an on-screen rendered vibrotactile line segment, either by the user placing their finger on the line and moving in a particular direction (Figure 7 left) or by moving their finger back and forth across the line and moving in a particular direction (Figure 7 right).

Building on the findings from experiments 1–3, three follow up studies were designed to investigate and identify the parameters that support accurate *line tracing* behavior. These data will be important for specifying new design guidelines to use when developing and using vibrotactile information in spatial contexts. Earlier evaluations with the VAI (Palani, 2013; Palani & Giudice, 2014, 2017) found that the ability to learn and mentally represent graphical material nonvisually via vibrotactile feedback is similar between blindfolded-sighted and BVI users. This finding is congruent with experiments 1–3, which also found no differences between blindfolded-sighted and BVI groups, suggesting that the ability to
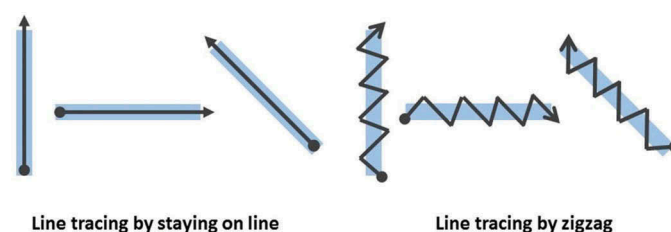

Line tracing by staying on line　　　　Line tracing by zigzag

Figure 7. Illustration of line tracing exploration strategy.

perform perceptual spatial tasks is similar between these participant demographics, irrespective of visual status. Given this similarity in performance, and our belief in the efficacy of this interface for also supporting eyes-free applications for sighted users, we argue that blindfolded-sighted participants serve as a reasonable representative sample for both groups when studying nonvisual performance with vibrotactile stimuli, as are studied here. Accordingly, evaluations in the subsequent experiments are primarily made with blindfolded-sighted participants. In order to validate our hypothesis that similar performance evidenced between groups on perceptual tasks will also manifest with the cognitive tasks investigated in experiments 4–6, and to ensure usability by both groups of potential end-users, we also conducted formative evaluations with BVI participants in these studies.

7. Experiment 4: Vibrotactile line tracing and orientation judgments

For guarantying accurate and efficient spatial behavior (e.g., path following or wayfinding), it is crucial for the user to be able to quickly and accurately trace the vibrotactile lines making up a complex map (i.e., transit path) and to also be able to correctly judge their orientation. The ability to judge individual line-orientations has been extensively described in the psychophysical literature with both vision and touch (for reviews, see Appelle, 1972; Baud-Bovy & Gentaz, 2012). This research has shown that perceptual variation occurs based on tangible line stimulus orientation and that participants are more accurate when predicting vertical or horizontal orientations over obliquely oriented stimuli. Although formal research has not been conducted on orientation judgments based on active exploration of vibrotactile lines, user feedback and informal observations from earlier studies from our group has revealed that people exhibit difficulty in tracing lines and detecting their orientation when they deviate from horizontal and vertical orientations (Gershon et al., 2016; Palani, Giudice, et al., 2018; Palani & Giudice, 2014). Accordingly, Experiment 4 was designed to assess users' ability to judge the orientation of individual vibrotactile lines rendered on touchscreen devices using one finger exploration. Building on Experiment 1, the study was also designed to simultaneously measure the minimum line width that best supports the cognitive process of line tracing behavior (as opposed to the perceptual process of line detection in Experiment 1) facilitated via touchscreen-based vibrotactile cuing.

7.1. Method

Eighteen blindfolded-sighted participants (9 females and 9 males, ages 18–33) were recruited for this experiment. In addition, four blind and visually-impaired (BVI) participants (3 males and 1 female, ages 28–43, BVI demographic details are presented in Appendix A) were recruited to ensure BVI usability with the task/stimuli. The stimulus set consisted of 36 different line-orientations represented as linear path segments. Each path was rendered at a unique orientation as part of a stimulus set of 36 orientations (i.e., 0° to 350° at 10° intervals). Findings from Experiment 1 suggested a 1 mm line

width for detection of vibrotactile lines. Since line tracing and orientation judgments require more complex behaviors than simple detection, it was unclear whether the detectable line width of 1 mm would be sufficient for this task. Hence, to determine the minimum line width that best supports accurate line tracing behavior and line-orientation judgments, the 36 line orientations were tested across 3 line widths (i.e., 1, 2, and 4 mm). The 36 line orientations and 3 line widths were balanced across 108 orientation judgment trials. Similar to experiment 3, all line stimuli the stimuli were presented using our prototype VAI (Palani, 2013) implemented on a tablet computer −10.1 inch Galaxy Table 3. As with the other experiments, the lines rendered were given a constant vibration based on Immersion Corp's UHL effect "Engine1_100" – an infinite repeating loop at 250 Hz with 100 percent power (Immersion Corp, 2019). The start and end of each line was indicated via additional synthetic speech output, using the device's built in TTS and speaker, indicating "Entrance" and "Exit" respectively. The user's finger movement behavior was tracked and logged within the device and subsequently used for measuring learning time.

7.2. Procedure

The study followed a within-subjects design with each participant performing 108 line tracing and line-orientation judgment trials. In each trial, participants started at the entrance of a simulated hallway at the center of the screen, which was indicated via an audio message and a tangible (2 mm) marker affixed to the screen. They then scanned the screen to: (1) identify the vibrotactile line and (2) trace the line until they reached its endpoint, indicated by an auditory message saying "exit". The device was then removed, and participants were asked to reconstruct the line-orientation from memory by physically adjusting a digital pointing device (Figure 8 right). Participants performed 2 practice trials and 3 learning-criterion trials before performing the 108 experimental trials (resulting in 792 observations for each tested line width and 66 observations for each tested orientation). During the practice session, the experimenter gave corrective feedback as necessary to ensure that participants fully understood the task. Participants then performed 3 learning-criterion trials where they had to trace an onscreen line segment and successfully reproduce the orientation of the perceived lines (i.e., within ± 10 degrees of error for the rendered line orientation).

Figure 8. Randomly generated oriented lines rendered on the experimental device and (right) the digital pointing device used for reproducing line orientation.

This criterion measure was implemented to ensure all participants were at an equivalent baseline before starting the experimental trials. Each participant took between 40 and 60 minutes to complete the entire experiment. Based on this design, line tracing times and accuracy in reproduced line orientations were compared between the 36 orientations and 3 line widths.

7.3. Results and discussion

A repeated measures ANOVA across the three line widths and 36 line-orientations revealed that the tracing time differed significantly based on the width of the rendered vibrotactile lines ($F(2, 105) = 12.619$, $p < .001$), but not on the orientation of the line ($F(35, 431) = 1.145$, $p > .05$). Post-hoc paired sample t-tests with Bonferroni correction revealed that the tracing time was significantly different ($p < .001$) between the three tested line widths, with 4 mm being the fastest and 1 mm being the slowest.

Similarly, an ANOVA revealed that reproduction accuracy significantly differed between the 36 line orientations ($F(35, 431) = 2.566$, $p < .001$), but no reliable differences were observed between the 3 line widths ($F(2, 105) = 0.805$, $p > .05$). The mean angular error across the 36 line-orientations (Figure 9) suggests that users were able to accurately judge vibrotactile line-orientation (as low as ~7°). Post-hoc paired sample t-tests with Bonferroni correction revealed that the reproduction accuracy was significantly different ($p < .001$) between the three tested line widths, with 4 mm lines being the most accurate.

Since BVI participants were employed here as a formative assessment to benchmark against the trend observed from the sighted group, the data from the BVI group was only analyzed descriptively. However, comparing the mean tracing times and angle reproduction accuracy between the two groups (Figure 9), suggests that the BVI group exhibited faster line tracing behavior and more accurate reproduction of line-orientation. While we a priori predicted similar results between group performances, the current results showing superior performance of BVI participants are not surprising, as this group is more familiar with haptic information extraction and learning and have also had prior experience using one finger for learning graphical information. Overall, Experiment 4 results suggest that rendering vibrotactile lines at a width of 4 mm best supports line tracing behavior and judgment of different line orientations. It should be noted that the superior performance with the 4 mm width is based on only tracing single straight-line segments. As such, this
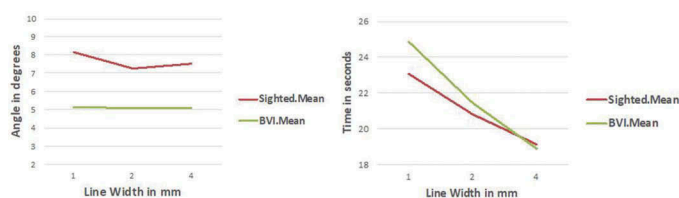
finding cannot be generalized to graphical materials comprised of multi-line segments. Experiment 5 extended the findings from this experiment to complex spatial path patterns comprising multi-segment lines.

8. Experiment 5: Building mental representations from spatial paths

Consider the sample scenario where users need to explore the subway map (Figure 1) using the vibro-audio interface and gain knowledge to plan a travel route. To successfully apprehend and build a globally coherent spatial image of this map (i.e., paths, stations, junctions, etc.,), users should be able to access and trace multiple line segments (i.e., transit lines) and understand the global connectivity between them. Toward this end, Experiment 5 was designed with a two-prong focus: (1) to evaluate users' ability to build a mental representation of multi-leg spatial path patterns, and (2) to empirically measure the minimum line width that best supports line tracing and integration of individual line segments into a globally coherent mental representation of the spatial paths. The three earlier experiments (1, 2, and 4) that compared different line widths have all shown a linear trend of increased performance with a corresponding increase in line width. While the widths established in each of these experiments hold true for the particular task tested, the earlier results on vibrotactile line width cannot be generalized to the more complex spatial learning task evaluated in this study. Hence, to understand the influence of line width on learning spatial path patterns and the subsequent development of mental representations, the four path patterns were tested across six different line widths (1, 2, 3, 4, 5, and 6 mm). We used a pattern-matching task to assess the accuracy of the developed mental representation using a response-based forced-choice procedure with a pre-defined stimulus set.

8.1. Method

Eighteen blindfolded-sighted participants (8 females and 10 males, ages 18–33) were recruited for this experiment. In addition, eight BVI participants (3 males and 5 females, ages 24–74) were also recruited as part of a formative assessment (BVI demographic details are presented in Appendix A). The stimulus set consisted of four different spatial path patterns. Each pattern comprised a start point, three legs (line segments) that were connected by two junctions (vertices), and an end point. The four paths were balanced for complexity in terms of line segment length, number of vertices, and leg orientation. For instance, path1 did not have any right-angled (90°) vertices, path2 only had right-angled (90°) vertices, path3 had one right-angled (90°) and one acute-angled (45°) vertex, and path4 had one right-angled (90°) and one obtuse-angled (135°) vertex.

The line widths for the stimuli set (1, 2, 3, 4, 5, and 6 mm) used a base width of 1 mm – as was found from Experiment 1 – and increased linearly up to 6 mm. The 6 line widths and 4 paths (see Figure 10) were balanced across 24 path matching trials. All 24 paths were rendered using the vibro-audio interface (VAI) implemented on a 5.6inch Galaxy Note4 Edge Android phablet (Palani, 2013). In each trial, the path

Figure 9. Mean angular error (left) and Mean tracing time (right) as a function of line width and participant groups.
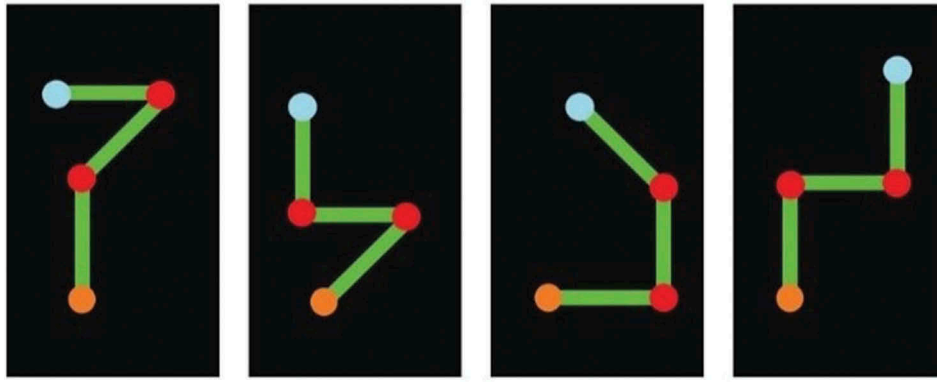
Figure 10. Experimental stimuli: four different path patterns.

segments were indicated using a constant vibratory feedback based on the Immersion Corp's UHL effect "Engine1_100" which uses a repeating loop at 250 Hz with 100% power (Immersion Corp, 2019). The start point, end point, and vertices were all indicated using a pulsing vibration based on the UHL effect "Weapon_1," which uses a wide-band 0.01 s pulse with a 50% duty cycle and a 0.02 sec period. In addition to vibrotactile feedback, the start point, end point, and two vertices were also indicated via speech output that stated, "Start", "End" and "Junction" respectively. The user's finger movement behavior was tracked and logged within the device and used for measuring learning time and analyzing tracing strategy.

8.2. Procedure

The study followed a within-subjects design where each participant performed 24 path learning trials (resulting in 108 observations for each pattern and 72 observations for each tested line width). In each trial, participants were asked to trace the spatial path once from the start point to the end point. Upon reaching the end, the device was removed. Participants were then asked to perform a spatial pattern matching task where they had to identify the just learned spatial path from three geometrically similar alternatives embossed on hardcopy paper. The three alternatives were the rotated and/or flipped versions of the correct pattern. Based on this design, the time taken to trace the entire path, the time spent on individual line segments, the time spent on vertices, and the accuracy in pattern matching were compared as a function of 4 paths and 6 line widths and across two participant groups (sighted and BVI).

8.3. Results and discussion

Tracing time here is interpreted as an indicator of spatio-cognitive effort required for perceiving and conceptualizing the spatial path pattern, i.e., longer tracing times indicate higher cognitive effort. A repeated measures ANOVA revealed that the tracing time differed significantly based on the width of the rendered vibrotactile lines ($F(5, 105) = 6.531$, $p < .001$). Post-hoc t-tests, based on Bonferroni correction, revealed that path tracing time was significantly worse with

1 mm and 2 mm line widths as compared to the other 4 line widths (see Table 7). However, differences were not statistically significant between the 3, 4, 5, and 6 mm line widths, indicating that a line width of 3 mm and above is effective for performing line tracing with vibrotactile cues. Similarly, the tracing time was significantly different between the four path patterns tested, independent of line width ($F(3, 428) = 4.41$, $p < .005$), with path4 (i.e., the path with one right-angled and one obtuse-angled vertex) yielding the lowest tracing time. Subsequent Bonferroni corrected post-hoc t-Tests between the time spent on vertices showed that participants spent significantly ($p < .05$) more time at vertices comprised of acute-angles (M = 29.59 sec) compared to those with obtuse-angles (M = 20.17 sec) or right-angles (M = 10.59 sec). This result is in line with the difference in tracing time between spatial path patterns, which showed that participants took the most time to trace paths with acute-angled vertices (i.e., path 1 and 3). This difficulty in tracing acute-angles is congruent with earlier research that compared angle perception between vibrotactile and electrostatic feedback on touchscreen devices (Gershon et al., 2016). Paired sample comparisons between the line tracing time for individual line segments, revealed that the tracing time for horizontal lines was significantly faster than for oriented lines ($t(251) = -2.146$, $p < .033$). While this is congruent with prior studies using traditional tangible media (Appelle, 1972), the tracing time for vertical lines did not reliably differ from oriented lines or the horizontal lines (all ps>0.05). These differences in tracing times for the three (i.e., horizontal, vertical, and slanted) lines could be attributed to the ergonomics of hand and finger positions. That is, participants had to bend/twist both their wrist and finger for tracing oriented paths. By contrast, tracing horizontal paths was

Table 7. Mean tracing time and standard deviation as a function of two participant groups.

Line Width (in mm)	Sighted		BVI	
	Mean (in seconds)	SD	Mean (in seconds)	SD
1	74.26	97.391	60.19	43.592
2	54.49	73.791	34	14.185
3	42.49	46.73	30.97	19.12
4	38.67	35.888	29.75	14.986
5	26.72	11.385	30.31	16.464
6	32.94	38.638	27.16	14.926

ergonomically easier as participants were only required to twist the wrist while tracing. For the pattern matching task, discrete scoring was applied based on the correctness of matching (i.e., 1 if correct, 0 otherwise). Findings from the ANOVA and post-hoc paired sample t-tests revealed that the line width did not statistically impact performance on matching accuracy (all ps>0.05). The matching accuracy for all tested line widths was above 95%, indicating that users were able to develop an accurate mental representation of the perceived patterns for all tested line widths.

The trend in the data from the sighted group was also observed for the BVI group (see Table 7). By descriptively comparing the mean tracing times between the two groups (Figure 11.), it is evident that the BVI group exhibited faster line tracing behavior. This trend is similar to Experiment 4 results, with the superior performance of BVI participants attributed to their greater familiarity with haptic learning.

Although the matching accuracy across all line widths was similar, chance performance for matching from four alternatives is 25%, representing less precision and greater probability of false positives than was present with the map reproduction and line identification measures used in our previous experiments. Corroborating these earlier findings in conjunction with findings from Experiment 4, it is suggested here that rendering vibrotactile lines at a width of 4 mm would best support users when employing exploratory procedures (Eps) supporting line tracing and apprehension of spatial path patterns via touchscreen-based vibrotactile feedback.

9. Experiment 6: Building mental representations of spatial path patterns using vibration as a warning cue

Previous studies have shown that a constant vibration on the fingertip can lead to sensory fatigue, limiting a user's ability to perceive vibratory cues over time (Craig, 1993; Raja, 2011). Indeed, a few participants in Experiment 5 and in earlier studies with the VAI (Palani et al., 2016; Palani & Giudice, 2017) have also self-reported that they felt numbness in the fingertip after tracing vibrotactile lines for a prolonged period (after ~45-60 minutes). Experiment 6 was designed to investigate the possibility of reversing the feedback mechanism of
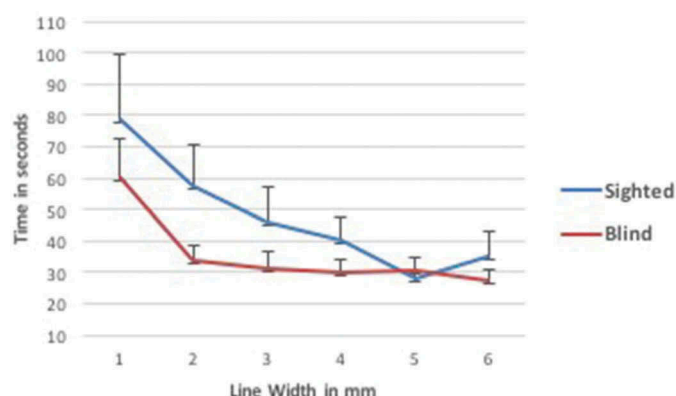
the interface by utilizing vibrotactile feedback as a negative-warning cue as opposed to a positive-guiding cue. This means, rather than following the path by tracing the vibrotactile cue representing the path itself, as was used in Experiment 5, participants here must try to trace the path, indicated by a negative "off" signal between the two vibrotactile lines. The experiment design was adopted from previous work by Loomis and colleagues which compared an Off-course and On-course vibrotactile cue mode for guiding users when walking a route using a handheld Haptic Pointer Interface, with results showing that indication of off-course vibrotactile feedback is sufficient for supporting route guidance behavior (Marston et al., 2007). For instance, imagine the subway map scenario again (Figure 1), where one has to learn the transit lines by feeling the borders of the path as opposed to feeling the path itself, as implemented in experiments 4 & 5. A similar example would be to follow a corridor path represented by the negative signal and feeling the two borders/walls along the corridor via vibrotactile feedback (see Figure 12).

Accordingly, Experiment 6 was designed with a two-fold objective: (1) to assess if users can develop an accurate mental representation of the presented spatial path pattern by using vibrotactile feedback as an off-path warning cue, and (2) to empirically measure the minimum interline-gap width that best supports line tracing and integration of individual line segments into a globally coherent spatial representation of the presented spatial path patterns.

9.1. Method

Eighteen blindfolded-sighted participants (8 females and 10 males, ages 18–28) were recruited for this experiment. Eight additional blind and visually-impaired (BVI) participants (3 males and 5 females, ages 24–74, were recruited for a formative assessment (BVI demographic details are presented in Appendix A). The structure and complexity of the four spatial path patterns used here were all similar to Experiment 5 (as shown in Figure 13). The only difference in the stimuli was that the paths (as shown in Figure 12) were rendered as a gap ("off" signal) between two bounding
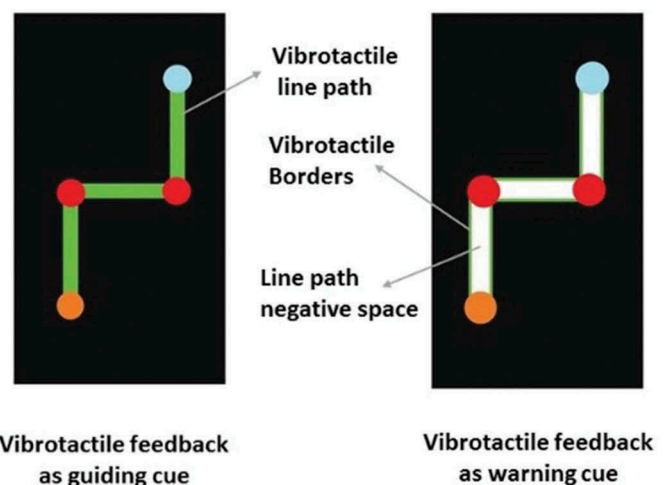

Figure 11. Mean tracing time as a function of line widths and participant groups.

Figure 12. Path tracing using vibrotactile lines versus vibrotactile borders.

Figure 13. Experimental Stimuli for path tracing: Four different spatial path patterns.

vibrotactile borders ("on" signal). Since the purpose of the borders are meant only to be an alert (i.e., detection task), a border width of 1 mm (based on findings from Experiment 1) was adopted for this design.

The actual path width (i.e., interline gap width) was adopted from Experiment 5, except for the 1 mm width, as findings from Experiment 2 suggested that vibrotactile lines (borders in this case) should be separated by a gap width of 2 mm or more to support discrimination of at least 75% accuracy. Accordingly, 5 different gap widths (i.e., the negative stimulus gap between the two vibrotactile borders) were adopted for this study. Together, the stimulus set comprised 5 gap widths starting from 2 mm and increasing by a factor of 1 up to 6 mm. Surprisingly, during pilot runs it was found that for the 2 and 3 mm gap widths, participants were unable to differentiate/identify the two borders that were comprised of 1 mm widths. As discussed earlier, this masking of the gap could be due to the spurious haptic perception caused by a system delay in triggering the vibratory feedback. Hence, to increase their saliency, a 2 mm border width was adopted for the 2 mm and 3 mm interline gaps and a 1 mm border width for the remaining three interline gaps. Furthermore, to evaluate the impact of having different border widths, the 4 mm gap width was considered twice: (1) with 1 mm borders, and (2) with 2 mm borders. The 5 and 6 mm gap widths were not included for this border width comparison, as 2 mm borders would eventually increase the aggregate width beyond 8 mm (a value known to consume excessive screen space based on previous work (Palani, 2013; Palani et al., 2016, p. 2018). Consequently, the final stimulus set was comprised of 6 different combinations of gap and border widths (2:2, 3:2, 4:1, 4:2, 5:1, 6:1). The 6 gap and border width combinations along with the 4 path patterns (see Figure 13) were all balanced across the 24 pattern matching trials. The apparatus and set-up (i.e., path patterns, vibratory, and auditory feedback) were the same as in Experiment 5. The only difference was that the gap was not indicated through any cues; instead, constant vibrotactile feedback was provided outside the bounding line areas, based on the Immersion Corp's UHL effect "Engine1_100" (i.e., 250 Hz with 100% power) was used to indicate the path borders (Immersion Corp, 2019).

9.2. Procedure

The study followed a within-subjects design where each participant performed 24 path learning trials (resulting in 108 observations for each pattern and 72 observations for each tested gap:border combination). In each trial, participants were asked to trace the spatial path once from the start point to the end point by staying within the two borders. Upon reaching the end point, the device was removed. Participants then performed a pattern matching task where they were asked to identify the just-learned spatial path from three geometrically similar alternatives embossed on hardcopy paper. Following the same design as Experiment 5, the time taken to trace the entire path pattern, the time spent on individual line segments, the time spent on vertices, and the accuracy in pattern matching was compared as a function of 4 patterns, 6 gap:border combinations and 2 participant groups (sighted versus BVI).

9.3. Results and discussion

Contrasting with Experiment 5, the path tracing time increased as a function of increasing gap width (see Figure 14). A repeated measures ANOVA revealed that the tracing time differed significantly as a function of the gap:border widths ($F (5, 120) = 3.4237$, $p < .01$) and that the path tracing times were significantly faster with paths using 2 mm borders as compared to 1 mm borders ($F(1, 430) = 6.60$, $p < .01$). The time spent at angled-vertices was similar to the results from Experiment 5, with participants spending significantly ($p < .05$) more time at vertices comprised of acute-angles ($M = 14.07$ sec) than at obtuse-angles ($M = 10.78$ sec) or right-angles ($M = 8.06$ sec). The temporal durations for tracing horizontal, vertical and slanted line segments were all significantly different from each other ($F(2, 807) = 3.870$, $p < .05$), with tracing of horizontal segments being the fastest and slanted lines as the slowest. As was discussed in Experiment 5, these temporal differences could be attributed to the ergonomics of hand and finger positions, but this hypothesis will require more experimentation to investigate further.

Post-hoc paired sample t-tests based on Bonferroni correction between gap widths showed that the tracing times with paths using 2 mm and 3 mm gap widths were significantly faster than that of the other three gap widths (all ps < 0.05). This outcome is contrary to the results from Experiment 2, which suggested 4 mm and above as the minimum interline gap for supporting discrimination of vibrotactile lines. This means that trials with 4, 5, and 6 mm gaps should have exhibited better performance when compared to 2 and 3 mm gap trials. To further investigate this assertion, the
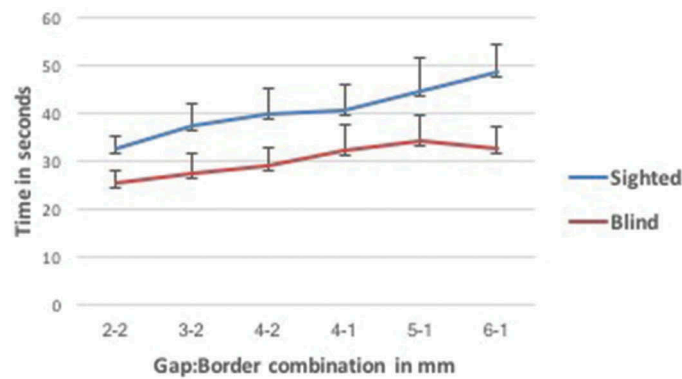
Figure 14. Tracing time as a function of gap:border widths and participant groups.

finger traces (based on the device log of user finger trajectories on the touchscreen) were analyzed and it was found that participants spent significantly more time outside the path borders as compared to touching the interline gap (t (359) = $-$ 3.016, $p < .003$). This finding suggests that, despite being deliberately instructed to stay within the two bounding vibrotactile lines and to use the vibration as a warning cue, participants relied primarily on the vibrotactile lines (i.e., borders) and scanned the path staying outside the intended path (i.e., interline gap). This reliance on vibrotactile borders likely explains the poor performance with 4, 5, and 6 mm gap trials, as the borders for these trials were rendered at 1 mm widths as opposed to the 2 mm wide borders used in the 2 and 3 mm gap trials. In addition to the wider borders, the 2 and 3 mm gaps were likely subthreshold for discrimination (as found in Experiment 2), meaning that there was a higher chance of users perceiving the two bounding lines as one vibrotactile line. We interpret these data as showing that participants were tracing the paths made of 2–2 and 3–2 gap:border combinations as line-based paths (i.e., ignoring the interline gaps and treating them as solid 4 mm and 5 mm line-paths); similar to how they traced the paths in Experiment 5. Adding support to this argument, the mean tracing time of maps with 2–2 and 3–2 gap:border combinations found here is similar to that of the 4 and 5 mm line widths tested in Experiment 5. With respect to matching performance, all six gap:border combinations exhibited above 95% matching accuracy, suggesting that participants were able to accurately develop a mental representation of the perceived path pattern. However, this high template matching accuracy, similar to Experiment 5, may have been elevated due to the low number of alternative path patterns (e.g., a 4-AFC task). Together, findings here suggest that

participants rely on vibrotactile feedback as a guidance cue even when instructed (and designed) to use them as a warning cue. Similar to experiments 4 & 5, BVI participants exhibited superior path tracing performance times (see Table 8 and Figure 14). Taken together, findings here, in conjunction with results from experiments 4 & 5, suggest that vibrotactile feedback is best implemented as a positive cue. If the situation demands implementation as a negative cue (e.g., to depict walls of a room), then a minimum line width of at least 2 mm should be maintained for supporting accurate and consistent detection of the bounding vibrotactile lines.

10. General discussion

The work presented in this paper was motivated by identifying perceptually-salient vibrotactile parameters and providing design guidelines for effective implementation of touchscreen-based haptic feedback using vibrotactile stimuli to support eyes-free interactions. In order to enable this nonvisual information access via haptic feedback (i.e., vibrotactile cues in the current evaluation), it is a pre-requisite that the presented graphical information is schematized and rendered based on: (1) maximizing the perceptual specificity of touchscreen-based vibrotactile feedback, and (2) recognizing the technical limitations of the interface that demands active exploration using just one finger for information extraction. To this end, six experiments were conducted with 64 blind participants and 105 blindfolded-sighted participants to empirically evaluate the necessary parameters and guidelines for schematization and rendering haptically perceivable graphical information on touchscreen devices. Based on the findings from these six studies, we have established six design guidelines for incorporating touchscreen-based vibrotactile

Table 8. Mean gap tracing time and standard deviation as a function of two participant groups.

Gap:border widths (mm)	Sighted		Blind	
Gap:border widths (mm)	Mean	SD	Mean	SD
2-2	32.36567	17.316975	25.18766	10.343877
3-2	37.06954	23.521407	27.23922	14.106367
4-2	39.71976	39.585541	29.02172	15.407677
4-1	40.31281	29.635404	31.99231	16.27907
5-1	44.50122	29.183822	34.10178	20.028749
6-1	48.33757	38.764066	32.457	18.111468

feedback as a primary modality and interaction style for non-visual information access. These guidelines will be helpful to designers and content providers who are creating digital materials or producing accessible graphics for many applications using the new class of haptic information-access technologies based on touchscreen-based devices.

10.1. Guideline 1. Minimum line width

For tasks requiring simple detection of graphical lines via vibrotactile cuing on touchscreen interfaces, each line should be rendered at a minimum width of 1 mm (as found in Exp-1). However, for supporting line discrimination and tracing, as is required for the successful utilization of important navigational tools like transit maps, the vibrotactile lines should be rendered at a minimum width of 4 mm (as found in Exp-2).

10.2. Guideline 2. Minimum separation

When rendering parallel vibrotactile lines on a touchscreen, as is often required with dense information like the transit map example, lines should be spatially separated with an interline gap of at least 4 mm, which maximizes the potential for each line to be perceived and identified as a distinct line (as found in Exp-2).

10.3. Guideline 3. Minimum angular separation

When rendering oriented and connected vibrotactile lines, as is required in the transit map example, oriented lines should be spatially separated from adjacent oriented lines using a minimum 4 mm cord length. This minimum cord length enables each oriented line to be clearly identified as distinct when users employ the common "circling" exploration strategy. While schematizing visual graphical materials for use with the VAI, in addition to rendering each line at a width of 4 mm as found in Exp-2, a minimum 4 mm angular separation (as found in Exp-3) should be maintained between any two oriented lines to aid in discrimination.

10.4. Guideline 4. Individual line-orientation

The orientation of any schematized vibrotactile line should remain as close as possible to the orientation of the original graphical line. Maintaining the line-orientation is crucial for the correct interpretation of many graphical materials such as line graphs, maps, statistical trends, etc. if the line-orientation has to be altered to facilitate haptic perception, a deviation of ±7° (as found in Exp-4) is acceptable. Altering the vibrotactile line up to ±7° will lead to a mental representation that is functionally equivalent to what is developed from perception of original visual line-orientations.

10.5. Guideline 5. Simplified intersections

Findings from Experiment 5 suggest that oriented vibrotactile lines can be accurately perceived even when rendered at intervals as low as 7°, provided the lines are of a width of at least 4 mm. Pertaining to common application, roadway intersections on traditional tangible graphics that rely on pressure-based stimulation are generally schematized based on a 8-sector model, where oriented lines are separated at 45° intervals (or a 16-sector model with 22.5° intervals). As stated in guideline 3, designers should consider schematizing intersections based on an understanding of which aspects (i.e., qualitative or quantitative) of the original intersection should be preserved after schematization. If precise quantitative information (e.g., the actual angle subtended between each intersecting line) has to be preserved, then designers should increase the overall size of the rendering to make the gap perceivable. If increasing the size of the graphic is not an option, then it is suggested here that the user be provided with supplementing audio/speech cues (e.g., speech output stating "a three-way intersection").

10.6. Guideline 6. Vibration feedback mechanism

Findings from Experiment 6 suggest that touchscreen-based vibratory feedback is best used as a positive-guiding cue rather than as a negative-warning cue. Results suggest that positive-guiding cues adhere to tracing strategies that naturally characterize user tracing behavior when extracting graphical information from touchscreen based devices. If technology designers and researchers choose to implement vibratory feedback as a negative-warning cue (e.g., to show the bounding lines of a region such as walls of a room), then a minimum line width of at least 2 mm should be maintained for accurate detection and effective tracing of the borders.

It should be noted that these six guidelines are not an exhaustive list of parameters for converting and rendering visual graphical lines into haptically perceivable equivalents on touchscreen interfaces. As stated in section 2.1, the guidelines provided here are based on a core graphical component (i.e., rectilinear lines) that serve as building blocks for extending this initial research program to other types of foundational graphical properties (such as regions, curved lines, points, etc.). However, findings with this core stimulus set clearly open the door to a new style of user interaction and information delivery supporting multitasking and a host of eyes-free applications due to situationally induced impairments and disabilities (SIID). Given the huge base of touchscreen usage (~ 2.8 billion touchscreen panels were shipped in 2016 alone (Statista, 2017)), the key usability parameters identified and established in this work will enhance the overall usability of touchscreen-based devices. We believe specification of these core guidelines will serve as basic building blocks and lay the foundation for future research aimed at development of new applications that support eyes-free interactions for use by both sighted and blind/visually impaired users.

ORCID

Hari P. Palani 🔸 http://orcid.org/0000-0002-3140-6359

References

Abdolrahmani, A., Kuber, R., & Hurst, A. (2016). An empirical investigation of the situationally-induced impairments experienced by blind mobile device users. *Proceedings of the 13th web for all conference on - W4A '16* (pp. 1–8). https://doi.org/http://doi.10.1145/2899475.2899482

Appelle, S. (1972). Perception and discrimination as a function of stimulus orientation: The "oblique effect" in man and animals. *Psychological Bulletin*, 78(4), 266–278. https://doi.org/http://doi.10.1037/h0033117

Apple Human Interface Guideline: Haptics. (2020). https://developer.apple.com/design/human-interface-guidelines/ios/user-interaction/haptics/

Apple Human Interface Guidelines: Visual Design. (2019). https://developer.apple.com/design/human-interface-guidelines/ios/visual-design/

Barfield, W. (2009). The use of haptic display technology in education. *Themes in Science and Technology Education*, 2(1–2), 11–30.

Barnard, L., Yi, J. S., Jacko, J. A., & Sears, A. (2007). Capturing the effects of context on human performance in mobile computing systems. *Personal and Ubiquitous Computing*, 11(2), 81–96. https://doi.org/10.1007/s00779-006-0063-x

Baud-Bovy, G., & Gentaz, E. (2012). The perception and representation of orientations: A study in the haptic modality. *Acta psychologica*, 141(1), 24–30. https://doi.org/10.1016/j.actpsy.2012.06.002

Bilton, N. (2013). *Disruptions: Visually impaired turn to smartphones to see their world. The New York Times.* http://bits.blogs.nytimes.com/2013/09/29/disruptions-guided-by-touch-screens-blind-turn-to-smartphones-for-sight/?_r=0

Bolanowski, S. J., Gescheider, G. A., Verrillo, R. T., & Checkosky, C. M. (1988). Four channels mediate the mechanical aspects of touch. *The Journal of the Acoustical Society of America*, 84(5), 1680–1694. https://doi.org/10.1121/1.397184

Braille Authority of North America. (2010). *Guidelines and standards for tactile graphics.* www.brailleauthority.org/tg

Butler, M., Holloway, L., Marriott, K., & Goncu, C. (2016). Understanding the graphical challenges faced by vision-impaired students in Australian universities. *Higher Education Research & Development*, 4360(August), 1–14. https://doi.org/http://doi.10.1080/07294360.2016.1177001

Buzzi, M. C., Buzzi, M., Donini, F., Leporini, B., & Paratore, M. T. (2013). Haptic reference cues to support the exploration of touchscreen mobile devices by blind users. In *Proceedings of the biannual conference of the italian chapter of SIGCHI* (Vol. 28). (CHItaly '13). ACM. https://doi-org.prxy4.ursus.maine.edu/10.1145/2499149.2499156

Carney, C., McGehee, D. V., Harland, K., Weiss, M., & Raby, M. (2016). *Using naturalistic driving data to examine teen driver behaviors present in motor vehicle crashes, 2007-2015.* AAA Foundation for Traffic Safety. https://aaafoundation.org/using-naturalistic-driving-data-examine-teen-driver-behaviors-present-motor-vehicle-crashes-2007-2015/

Challis, B. (2013). Tactile interaction. The Encyclopedia of Human-Computer Interaction, 2nd Ed.

Chiasson, J., McGrath, B., & Rupert, A. (2003). Enhanced situation awareness in sea, air and land environments. In *North atlantic treaty organization's RTO meeting proceedings 86* (pp. 347–356). https://www.researchgate.net/publication/235146416_Enhanced_Situation_Awareness_in_Sea_Air_and_Land_Environments

Choe, W., & Lee, M. W. (2015). Discomfort glare model for mobile display. *2015 IEEE 5th international conference on consumer electronics - Berlin (ICCE-Berlin)* (pp. 471–473). https://doi.org/http://doi.10.1109/ICCE-Berlin.2015.7391313

Choi, S., & Kuchenbecker, K. J. (2013). Vibrotactile display: Perception, technology, and applications. *Proceedings of the IEEE*, 101(9), 2093–2104. https://doi.org/10.1109/JPROC.2012.2221071

Cohen, J. (1988). *Statistical power analysis for the behavioral sciences* (2nd ed.). Erlbaum Associates.

Craig, J. C. (1993). Anomalous sensations following prolonged tactile stimulation. *Neuropsychologia*, 31(3), 277–291. https://doi.org/10.1016/0028-3932(93)90092-E

Faul, F., Erdfelder, E., Lang, A.-G., & Buchner, A. (2007). G* Power 3: A flexible statistical power analysis program for the social, behavioral, and biomedical sciences. *Behavior Research Methods*, 39(2), 175–191. https://doi.org/10.3758/BF03193146

Gershon, P., Klatzky, R. L., Palani, H. P., & Giudice, N. A. (2016). Visual, tangible, and touch-screen: comparison of platforms for displaying simple graphics. *Assistive Technology*, 28(1), 1–6. https://doi.org/10.1080/10400435.2015.1054566

Giudice, N. A., Betty, M. R., & Loomis, J. M. (2011). Functional equivalence of spatial images from touch and vision: Evidence from spatial updating in blind and sighted individuals. *Journal of Experimental Psychology. Learning, Memory, and Cognition*, 37(3), 621–634. https://doi.org/http://doi.10.1037/a0022331

Giudice, N. A., Klatzky, R. L., & Loomis, J. M. (2009). Evidence for amodal representations after bimodal learning: integration of haptic-visual layouts into a common spatial image. *Spatial Cognition & Computation*, 9(4), 287–304. https://doi.org/10.1080/13875860903305664

Giudice, N. A., Palani, H. P., Brenner, E., & Kramer, K. M. (2012). Learning non-visual graphical information using a touch-based vibro-audio interface. In *Proc.14th Int. ACM SIGACCESS conference on Computers and accessibility* (pp. 103–110). ACM Press. https://doi.org/http://doi.10.1145/2384916.2384935

Goncu, C., & Marriott, K. (2011). GraVVITAS: Generic multi-touch presentation of accessible graphics. *Lecture Notes in Computer Science*, 6946, 30–48. https://doi.org/http://doi.10.1007/978-3-642-23774-4_5

Grow, D. I., Verner, L. N., & Okamura, A. M. (2007). *Educational haptics. AAAI spring symposium: Semantic scientific knowledge integration.* https://pdfs.semanticscholar.org/aeee/8e3f58e384cbd652c34bbfe18347b587d5f8.pdf?_ga= 2.237210304.1561149690.1568562388-1085281903.1568222523

Grussenmeyer, W., & Folmer, E. (2017). Accessible touchscreen technology for people with visual impairments: A survey. *ACM Transactions on Accessible Computing (TACCESS)*, 9(2), 31. https://doi.org/10.1145/3022701

Hayward, V., Astley, O. R., Cruz-Hernandez, M., Grant, D., & Robles-De-La-Torre, G. (2004). Haptic interfaces and devices. *Sensor Review*, 24(1), 16–29. https://doi.org/10.1108/02602280410515770

Immersion Corp. (2019). www.immersion.com

Klatzky, R. L., Giudice, N. A., Bennett, C. R., & Loomis, J. M. (2014). Touch-screen technology for the dynamic display of 2D spatial information without vision: Promise and progress. *Multisensory Research*, 27(5–6), 359–378. https://doi.org/10.1163/22134808-00002447

Lederman, S. J., & Klatzky, R. L. (1987). Hand movements: A window into haptic object recognition. *Cognitive Psychology*, 19(3), 342–368. https://doi.org/10.1016/0010-0285(87)90008-9

Lederman, S. J., & Klatzky, R. L. (2009). Haptic perception: A Tutorial. *Attention, Perception & Psychophysics*, 71(7), 1439–1459. https://doi.org/10.3758/APP.71.7.1439

Leung, R., MacLean, K., Bertelsen, M. B., & Saubhasik, M. (2007). Evaluation of haptically augmented touchscreen gui elements under cognitive load. *Proceedings of the Ninth International Conference on Multimodal Interfaces ICMI 07*, 7, 374–381. https://doi.org/10.1145/1322192.1322258

Loomis, J. M., Klatzky, R. L., & Giudice, N. A. (2013). Representing 3D space in working memory: Spatial images from vision, hearing, touch, and language. In *Multisensory imagery* (pp. 131–155). Springer.

Loomis, J. M., & Lederman, S. J. (1986). Tactual Perception. *Handbook of Perception and Human Performances*, 2(31), 2.

Maclean, K. (2008). Haptic interaction design for everyday interfaces. *Reviews of Human Factors and Ergonomics*, 4(1), 149–194. https://doi.org/10.1518/155723408X342826

Marston, J. R., Loomis, J. M., Klatzky, R. L., & Golledge, R. G. (2007). Nonvisual route following with guidance from a simple haptic or auditory display. *Journal of Visual Impairment & Blindness*, 101 (4), 203–211. http://www.psy.cmu.edu:16080/faculty/klatzky/07Marston et al JVIB .pdf

Miller, G. A. (1956). The magical number seven, plus or minus two: Some limits on our capacity for processing information. *Psychological Review*, 63, 2. https://doi.org/10.1037/h0043158

Monares, A., Ochoa, S. F., Pino, J. A., Herskovic, V., Rodriguez-Covili, J., & Neyem, A. (2011). Mobile computing in urban emergency situations: Improving the support to firefighters in the field. *Expert Systems with Applications*, 38(2), 1255–1267. https://doi.org/10.1016/j.eswa.2010.05.018

Mullenbach, J., Shultz, C., Colgate, J. E., & Piper, A. M. (2014). Exploring affective communication through variable - friction surface haptics. In *Proc. SIGCHI conference on human factors in computing systems* (pp. 3963–3972).

Ng, A., Brewster, S., & Crossan, A. (2011). The effects of encumbrance on mobile gesture interactions. In *Proceedings of the 13th international conference on human computer interaction with mobile devices and services, mobileHCI*.

O'Modhrain, S., Giudice, N. A., Gardner, J. A., & Legge, G. E. (2015). designing media for visually-impaired users of refreshable touch displays: Possibilities and Pitfalls. *IEEE Transactions on Haptics*, 8(3), 248–257. https://doi.org/10.1109/TOH.2015.2466231

Palani, H. P. (2013). *Making graphical information accessible without vision using touch-based devices* [Unpublished Master's Thesis]. University of Maine.

Palani, H. P. (2018). *Principles and guidelines for advancement of touchscreen-based non-visual access to 2D spatial information* [Unpublished Dissertation]. University of Maine.

Palani, H. P., Giudice, G. B., & Giudice, N. A. (2018). Haptic information access using touchscreen devices: Design guidelines for accurate perception of angular magnitude and line orientation. In *Universal access in human-computer interaction. methods, technologies, and users, UAHCI 2018* (pp. 243–255). Springer International Publishing. https://doi.org/10.1007/978-3-319-92049-8_18

Palani, H. P., & Giudice, N. A. (2014). Evaluation of non-visual panning operations using touch-screen devices. In *Proc. 16th Int. ACM SIGACCESS conference on Computers & accessibility*. ACM.

Palani, H. P., & Giudice, N. A. (2017). Principles for designing large-format refreshable haptic graphics using touchscreen devices. *ACM Transactions on Accessible Computing*, 9(3), 1–25. https://doi.org/10.1145/3035537

Palani, H. P., Giudice, U., & Giudice, N. A. (2016). Evaluation of Non-visual zooming operations on touchscreen devices. In *Universal access in human-computer interaction. interaction techniques and environments: 10th international conference, UAHCI 2016, held as part of HCI international 2016, Toronto, ON, Canada, July 17- 22,2016, proceedings, part II* (pp. 162–174). Springer International Publishing.

Palani, H. P., Tennison, J. L., & Giudice, N. A. (2018). Touchscreen-based haptic information access for assisting blind and visually-impaired users: Perceptual parameters and design guidelines. In *9th international conference on applied human factors and ergonomics*.

Pitts, M. J., Skrypchuk, L., Wellings, T., Attridge, A., & Williams, M. A. (2012). Evaluating user response to in-car haptic feedback touchscreens using the lane change test. In *Advances in human-computer interaction, 2012*. https://doi.org/10.1155/2012/598739

Precision Microdrives. (2016). *Product data sheet: Precision haptic 13mm linear resonant actuator—3mm type.*https://www.precisionmicrodrives.com/wp-content/uploads/2016/04/C13-000-datasheet.pdf

Raja, M. K. (2011). *The development and validation of a new smartphone based non-visual spatial interface for learning indoor layouts* [unpublished master's thesis]. University of Maine.

Rao, S. (2012). *High-definition haptics: Feel the difference!* Texas Instruments Analog Applications Journal. https://www.ti.com/lit/an/slyt483/slyt483.pdf

Rodriguez, R. G., Garretón, J. A. Y., & Pattini, A. E. (2016). Glare and cognitive performance in screen work in the presence of sunlight. *Lighting Research & Technology*, 48(2), 221–238. https://doi.org/10.1177/1477153515577851

Rowell, J., & Ungar, S. (2003). The world of touch: results of an international survey of tactile maps and symbols. *Cartographic Journal, The*, 40(3), 259–263. https://doi.org/10.1179/000870403225012961

Sathian, K. (1998). Perceptual learning. *Current Science*, Sep(10), 451–457.

Schieber, F. (2006). Vision and Aging. In J. E. Birren & K. W. Schaire (Eds..), *Handbook of the psychology of aging* (pp. 129–161). Elsevier. http://dx.doi.10.1016/B978-012101264-9/50010-0

Sears, A., Lin, M., Jacko, J., & Xiao, Y. (2003). When computers fade: Pervasive computing and situationally-induced impairments and disabilities. *HCI International*, 2(3), 1298–1302.

Shakeri, G., Ng, A., Williamson, J. H., & Brewster, S. A. (2016). Evaluation of haptic patterns on a steering wheel. *Proceedings of the 8th international conference on automotive user interfaces and interactive vehicular applications - automotive'ui 16* (pp. 129–136). https://doi.org/10.1145/3003715.3005417

Sjostrom, C. (2001). Using haptics in computer interfaces for blind people. In *CHI '01 extended abstracts on human factors in computing systems* (pp. 245–246). (CHI EA '01). ACM.https://doi.org/10.1145/634067.634213

Statista. (2017). *Touchscreen usage.* http://www.statista.com/statistics/259983/global-shipment-forecast-for-touch-screen-displays/

Su, J., Rosenzweig, A., Goel, A., de Lara, E., & Truong, K. N. (2010). Timbremap: Enabling the visually-impaired to use maps on touch-enabled devices. In *Proceedings of the 12th international conference on Human computer interaction with mobile devices and services* (pp. 17–26). ACM. http://portal.acm.org/citation.cfm?id=1851606

Swette, R., May, K. R., Gable, T. M., & Walker, B. N. (2013). Comparing three novel multimodal touch interfaces for infotainment menus. In *Proceedings of the 5th international conference on automotive user interfaces and interactive vehicular applications - automotiveUI '13* (pp. 100–107). https://doi.org/10.1145/2516540.2516559

Tennison, J. L., & Gorlewicz, J. L. (2016). Toward non-visual graphics representations on vibratory touchscreens: shape exploration and identification. In F. Bello, H. Kajimoto, & Y. Visell (Eds.), *Haptics: perception, devices, control, and applications: 10th international conference, eurohaptics 2016, London, UK, July 4-7, 2016, proceedings, part II* (pp. 384–395). Springer International Publishing. https://doi.org/10.1007/978-3-319-42324-1_38

Vatavu, R. (2017). Visual impairments and mobile touchscreen interaction: state-of-the-art, causes of visual impairment, and design guidelines. *International Journal of Human-computer Interaction*, 33(6), 486–509. https://doi.org/10.1080/10447318.2017.1279827

Wickens, C. D., & Seppelt, B. (2002). Interference with driving or in-vehicle task information: The effects of auditory versus visual delivery. University of Illinois, Aviation Human Factors Division.

Xu, C., Israr, A., Poupyrev, I., Bau, O., & Harrison, C. (2011). Tactile display for the visually impaired using TeslaTouch.*Proc.CHI EA '11*, 317–322. https://doi.org/10.1145/1979742.1979705

Zion Market Research. (2019). *Multi-touch screen market by product (smartphones, tablets, laptops, televisions, kiosks, and large interactive screens), by technology (resistive, capacitive, infrared, optical, and others), and by application (infotainment, enterprises, entertainment, and others): global industry perspective, comprehensive analysis, and forecast, 2018–2025.* https://www.zionmarketresearch.com/report/multi-touch-screens-market

About the Authors

Hari P. Palani received his PhD degree in Spatial Informatics from the University of Maine. He is the Founder and Chief Executive Office of UNAR Labs. His research interests include haptic perception, multimodal interface design, spatial cognition and nonvisual graphic accessibility.

Paul D. S. Fink, is a Ph.D. student in Spatial Information Science and Engineering at the University of Maine. His research intersects user experience, technology education, and accessibility. Current work includes designing a virtual learning platform for autonomous vehicle AI research and development.

Nicholas A. Giudice is a Professor in the School of Computing and Information Science, University of Maine. His research combines techniques from Experimental Psychology and Human-Computer Interaction, with expertise in spatial learning and navigation and in the design and evaluation of multimodal information-access technologies for blind and visually impaired users.

Appendix. Demographic details of blind and visually-impaired participants

Blind participant information from Experiment 1

Sex	Etiology of Blindness	Residual Vision	Age	Onset	Years (stable)
M	Retinopathy of prematurity	None	18	Birth	18
F	Retinitis pigmentosa	Light Perception	21	Age 7	14
F	Retinitis pigmentosa	None	22	Birth	22
M	Retinopathy of prematurity	None	24	Birth	24
F	Leber's congenital amaurosis	Light Perception	43	Birth	43
M	Leber's congenital amaurosis	Light Perception	40	Birth	40
F	Pathological Myopia	Light/dark perception in right eye, Fuzzy colors	57	Age 42	15
F	Retinopathy of Prematurity	None	74	Birth	74
M	Retinitis Pigmentosa, atypical, with cone dystrophy	Light/dark perception, some functional peripheral	58	Age 25	23
F	Retinitis Pigmentose	Light/dark perception	63	Age 11	52
M	Retinopathy of Prematurity	Light/dark perception	44	Birth	44
F	Retinopathy of Prematurity	Light/dark perception	71	Birth	71
F	Retinopathy of Prematurity	Light/dark perception	56	Birth	56
M	Retinitis Pigmentose	Light/dark perception	63	Birth	63
M	Glaucoma	Light dark perception	21	Age 16	5
F	Unknown	Light/dark perception	29	Age 17	12
F	Congential Cataracts, Glaucoma	Light/dark perception	70	Age 50	20
M	Retinopathy of Prematurity	Light/dark perception	31	Birth	31
M	Retinopathy of Prematurity	Light/dark perception	43	Birth	43
F	Retinitis Pigmentose	Light/dark perception	37	Birth	37

Blind participant information from Experiment 2

Sex	Etiology of Blindness	Residual Vision	Age	Onset	Years (stable)
F	Retinitis pigmentosa	Light Perception	20	Age 7	13
F	Retinitis pigmentosa	None	22	Birth	22
M	Retinopathy of prematurity	None	24	Birth	24
F	Leber's congenital amaurosis	Light Perception	43	Birth	43
M	Leber's congenital amaurosis	Light Perception	40	Birth	40
F	Pathological Myopia	Light/dark perception in right eye, Fuzzy colors	57	Age 42	15
F	Retinopathy of Prematurity	None	74	Birth	74
M	Retinitis Pigmentosa, atypical, with cone dystrophy	Light/dark perception, some functional peripheral	58	Age 25	23
F	Retinitis Pigmentose	Light/dark perception	63	Age 11	52
M	Retinopathy of Prematurity	Light/dark perception	44	Birth	44
F	Retinopathy of Prematurity	Light/dark perception	71	Birth	71
F	Retinopathy of Prematurity	Light/dark perception	56	Birth	56
M	Retinitis Pigmentose	Light/dark perception	63	Birth	63
M	Glaucoma	Light dark perception	21	Age 16	5
F	Unknown	Light/dark perception	29	Age 17	12
F	Congential Cataracts, Glaucoma	Light/dark perception	70	Age 50	20
M	Retinopathy of Prematurity	Light/dark perception	31	Birth	31
F	Retinitis Pigmentose	Light/dark perception	37	Birth	37

Blind participant information from Experiment 3

Sex	Etiology of Blindness	Residual Vision	Age	Onset	Years (stable)
M	Retinopathy of prematurity	None	24	Birth	24
F	Leber's congenital amaurosis	Light Perception	43	Birth	43
M	Leber's congenital amaurosis	Light Perception	40	Birth	40
F	Pathological Myopia	Light/dark perception in right eye, Fuzzy colors	57	Age 42	15
F	Retinopathy of Prematurity	None	74	Birth	74
M	Retinitis Pigmentosa	Light/dark perception, some functional peripheral	58	Age 25	23
F	Retinitis Pigmentose	Light/dark perception	63	Age 11	52
F	Retinopathy of Prematurity	Light/dark perception	71	Birth	71

Blind participant information from Experiment 4

Sex	Etiology of Blindness	Residual Vision	Age	Onset	Years (stable)
M	Retinopathy of Prematurity	Light/dark perception	31	Birth	31
M	Retinopathy of Prematurity	Light/dark perception	43	Birth	43
F	Retinitis Pigmentose	Light/dark perception	37	Birth	37
M	Retinopathy of prematurity	None	28	Birth	28

Blind participant information from Experiment 5 & 6

Sex	Etiology of Blindness	Residual Vision	Age	Onset	Years (stable)
M	Retinopathy of prematurity	None	24	Birth	24
F	Leber's congenital amaurosis	Light Perception	43	Birth	43
M	Leber's congenital amaurosis	Light Perception	40	Birth	40
F	Pathological Myopia	Light/dark perception in right eye, Fuzzy colors	57	Age 42	15
F	Retinopathy of Prematurity	None	74	Birth	74
M	Retinitis Pigmentosa, atypical, with cone dystrophy	Light/dark perception, some functional peripheral	58	Age 25	23
F	Retinitis Pigmentose	Light/dark perception	63	Age 11	52
F	Retinopathy of Prematurity	Light/dark perception	71	Birth	71